

THE UNIVERSITY OF CALGARY

GPS SINGLE DIFFERENCE MODEL STUDIES

BY

KENT W. POINTON

A THESIS

SUBMITTED TO THE FACULTY OF GRADUATE STUDIES  
IN PARTIAL FULFILLMENT OF THE REQUIREMENTS FOR THE  
DEGREE OF MASTER OF SCIENCE

DEPARTMENT OF SURVEYING ENGINEERING

CALGARY, ALBERTA

MARCH, 1989

© KENT W. POINTON, 1989

**THE UNIVERSITY OF CALGARY**  
**FACULTY OF GRADUATE STUDIES**

The undersigned certify that they have read, and recommend to the Faculty of Graduate Studies for acceptance, a thesis entitled "GPS Single Difference Model Studies," submitted by Kent Whitfield Pointon in partial fulfillment of the degree of Master of Science.

*K.P. Schwarz*

\_\_\_\_\_  
Chairman, Dr. K.P. Schwarz  
Department of Surveying Engineering

*E.J. Krakiwsky*  
\_\_\_\_\_  
Dr. E.J. Krakiwsky  
Department of Surveying Engineering

*G. Lachapelle*  
\_\_\_\_\_  
Dr. G. Lachapelle  
Department of Surveying Engineering

*D.M. Lintock*  
\_\_\_\_\_  
Dr. D. ~~Mc~~Lintock  
Shell Canada Limited

*J.F. Morrall*  
\_\_\_\_\_  
Dr. J.F. Morrall  
Department of Civil Engineering

Date 13.3.1989

## ABSTRACT

The original University of Calgary single difference GPS data processing package, ASTRO, was developed and tested using only simulated orbit and phase data. The first objective of this thesis was to make the program work with observed data. The second objective was to determine if the use of the single difference observable is a viable approach to precise GPS positioning. To fulfill the second objective, a series of model enhancements had to be implemented to improve the performance of the ASTRO program. The enhancements are mainly to the receiver clock model.

To make the program run with observed data, a method of determining the six Keplerian initial conditions from the broadcast ephemeris had to be developed. The initial conditions are used in the numerical integration routines which compute the satellite positions. A difference of less than two metres between the broadcast ephemeris and integrated orbit has been obtained.

Adjustments with the original version of the ASTRO program gave rather poor results. A large systematic trend in the residuals, representing unmodelled receiver clock biases, is a major contributor to the poor results. An

inherent instability in the single difference model has also been identified.

A first-order Gauss-Markov process has been implemented to absorb the systematic trend. In addition, the receiver clock model has been revised to account for time-tag errors and the facility to treat the ambiguities as weighted parameters has been added. Baseline length errors of under a few parts per million have been obtained but only when the ambiguities are held fixed and short correlation times (120 seconds) are used in the random process. If longer correlation times are used, interaction between the receiver clock polynomials and the random process prevents proper convergence of the adjustment. Treating the ambiguities as weighted parameters, both with and without incorporating the Markov process, also produces convergence problems. This instability problem has not been successfully resolved.

The requirement of accurate a priori knowledge of the ambiguities is a significant constraint on the usefulness of the program. In addition, it is felt that the receiver clock models currently implemented are not the optimal solution to the clock problem. At present, the single difference models investigated in this thesis cannot be considered as a viable alternative to double difference adjustments.

## ACKNOWLEDGEMENTS

I wish to express my gratitude to my supervisor, Dr. K.P. Schwarz for his support and encouragement throughout the course of this study. His advise has proved invaluable to the completion of this thesis.

I have also had the benefit of many valuable discussions with Dr. E.J. Krakiwsky, Dr. I.N. Tziavos and M.E. Cannon on aspects of GPS positioning. I would also like to acknowledge my fellow graduate students with whom I have had many useful debates.

This research has been funded in part by a Natural Science and Engineering Research Council Postgraduate Scholarship plus financial support in the form of a EDO Canada 1987 Scholarship and the University of Calgary Graduate Assistantships.

I am also grateful to my wife, Dianne Allen and my new daughter, Twila for sharing the joys and trials of graduate studies with me.

## TABLE OF CONTENTS

<b>Abstract</b>	<b>iii</b>
<b>Acknowledgements</b>	<b>v</b>
<b>Table of Contents</b>	<b>vi</b>
<b>List of Tables</b>	<b>viii</b>
<b>List of Figures</b>	<b>ix</b>
<b>1 Introduction</b>	<b>1</b>
1.1 Objectives and Outline of the Thesis.....	3
1.2 Layout of the Test Network.....	6
1.3 Data Preprocessor and Cycle Slip Correction Programs.....	9
<b>2 Bias Modelling</b>	<b>15</b>
2.1 A Review of the Phase Observation Equations....	16
2.2 Receiver Clock Modelling.....	19
2.3 Atmospheric Propagation Delay Modelling.....	26
2.4 ASTRO Adjustment Software.....	28
<b>3 Computation of the Keplerian Initial Conditions     from the Broadcast Ephemeris.</b>	<b>32</b>
3.1 Review of the Broadcast Ephemeris.....	33
3.2 Method of Computing the Keplerian Initial Conditions.....	34
3.3 Comparison of the Satellite Coordinates from the Broadcast Ephemeris and Estimated Initial Conditions.....	39
<b>4 Positioning Results Without Model Refinements</b>	<b>48</b>
4.1 Initial Results on All Baselines.....	49

<b>5</b>	<b>Positioning Results with Model Variations</b>	<b>58</b>
5.1	Revised Polynomial Receiver Clock Model.....	58
5.2	Adjustments with Weighted Ambiguities.....	67
5.3	Gauss-Markov Receiver Clock Model.....	70
5.3.1	Discussion of the Autocorrelation Function and Gauss-Markov Processes.....	71
5.3.2	Initial Baseline Results with a Gauss- Markov Model Implemented.....	75
<b>6</b>	<b>Double Difference Adjustments</b>	<b>87</b>
6.1	Double Difference Adjustment Results, Version 1.....	88
6.2	Double Difference Adjustment Results, Version 2.....	92
<b>7</b>	<b>Conclusions and Recommendations</b>	<b>98</b>
	<b>References</b>	<b>105</b>
	<b>Appendix A</b>	<b>110</b>

## LIST OF TABLES

3.1	Mean Coordinate and Velocity Differences.....	41
3.2	Estimates of the Keplerian Initial Conditions; Satellite PRN 13.....	41
3.3	Estimates of the Keplerian Initial Conditions; Satellite PRN 12.....	42
3.4	Estimates of the Keplerian Initial Conditions; Satellite PRN 9.....	42
4.1	Baseline Errors from Initial Runs.....	51
4.2	Correlation Coefficient Matrix for Run 4.1, Baseline ROOF to CATA.....	56
5.1	Baseline Errors from Adjustments With An Updated Polynomial Receiver Clock Model.....	60
5.2	Correlation Coefficient Matrix for Run 5.1, Baseline ROOF to CATA.....	62
5.3	Correlation Coefficient Matrix for Run 5.5, Baseline ROOF to CATA.....	65
5.4	Baseline Errors from Adjustments With Weighted Ambiguities.....	69
5.5	Baseline Errors from Adjustments with a Gauss-Markov Process Implemented.....	79
5.6	Correlation Coefficient Matrix for Run 5.9, Baseline ROOF to CATA.....	80
6.1	Baseline Errors from Version 1 Double Difference Adjustments.....	89
6.2	Correlation Coefficient Matrix for Run 6.1, Baseline ROOF to CATA.....	91
6.3	Baseline Errors from Version 2 Double Difference Adjustments.....	93

## LIST OF FIGURES

1.1	Layout of the Test Network.....	7
1.2	GDOP Throughout the Observation Session.....	8
1.3	Preprocessor Data Flow Diagram.....	10
1.4	Cycle Slip Removal Flow Chart.....	12
3.1	Satellite Position Errors; First Estimate.....	40
3.2	Satellite Position Errors; Second Estimate.....	44
3.3	Satellite Position Errors; Final Estimate.....	46
4.1	Residuals from the Adjustment of Baseline ROOF to CATA.....	52
4.2	Residuals from the Adjustment of Baseline ROOF to METC.....	53
4.3	Residuals from the Adjustment of Baseline METC to CATA.....	54
5.1	Residuals from the Adjustment of Baseline ROOF to CATA, Run 5.6.....	66
5.2	Autocorrelation Function of Satellite 13 Residuals, ROOF to CATA Fixed Stations Adjustment..	76
5.3	Residuals from the Adjustment of Baseline ROOF to CATA with a Gauss-Markov Clock Model.....	81
5.4	Residuals from the Run 5.11 Adjustment.....	83
6.1	Residuals from the Double Difference Adjustment of Baseline ROOF to CATA, Run 6.1.....	90
6.2	Residuals from the Double Difference Adjustment of Baseline ROOF to CATA, Run 6.2.....	94
6.4	Comparison of the Residuals from Runs 6.2 and 6.3, Satellite Combination 13-11.....	96

# CHAPTER 1

## INTRODUCTION

Over the past decade, the development and utilization of GPS positioning techniques for the precise measurement of geodetic baselines and geodynamic studies has been an active area of research. Baseline measurement accuracies of a few parts per million are currently being achieved using single frequency receivers and processing software with no orbit improvement capabilities, see e.g. Lachapelle and Cannon, 1986; Langley et al., 1986; Jones and Larden, 1987; McArthur, 1987. Accuracies of 0.1 ppm or better, required for geodynamic studies (Hothem and Williams, 1985; Pointon et al., 1987) have been demonstrated on longer lines with improved modelling of the major error sources and dual frequency receivers, see e.g. Bock et al., 1986; Beutler et al., 1987a. Efforts are in progress to achieve accuracies in the  $10^{-8}$  range. This requires carefully designed experiments on networks of widely spaced observing stations with special efforts to reduce orbital errors, high performance dual frequency GPS receivers with stable atomic clocks and reliable atmospheric information.

Most of these results have been achieved using double difference techniques for the carrier phase. These techniques have major advantages in terms of economy and stability of the numerical process. They have, however, drawbacks in reducing the information content of the data. Forming double differences cancels the common orbit errors and the receiver clock errors which are explicitly modelled in the single difference observation equation. Cancelling the biases is undesirable when orbit improvement is to be carried out since the observation will be less sensitive to orbital errors (Langley et al., 1984; Nakiboglu et al., 1985). Also, the receiver clock errors are in fact only partially removed by differencing. The remaining clock errors must be further modelled, otherwise the effect will be absorbed in the estimates of the other parameters.

The research group at The University of Calgary developed a program package to provide GPS positioning at the 0.1 ppm level using single differences. It was used to evaluate permanent tracking station locations for a regional network extending over the Canadian territory using simulated data. The results of this analysis can be found in Buffett (1985), Nakiboglu et al., (1985) and Wanless (1985). Further research has gone into developing the concept of a network of permanent tracking stations, known as the Active

Control System in Canada (Delikaraoglou et al., 1986), and as the fiducial concept in The United States (Davidson et al., 1986).

The University of Calgary program package, originally known as ASTRO, provided for the simultaneous adjustment of ground station coordinates for a network of observing stations plus orbital improvement. Common biases such as orbital errors, unaccounted for tropospheric refraction and receiver clock biases are explicitly modelled. Single difference observations (between stations) are chosen as the basic observational unit; thus, satellite clock errors and the common part of the atmospheric biases and orbital errors are differenced away. Modelling of the remaining biases allows for tuning of the a priori variance information to provide an optimal solution. This package provides an interesting alternative to the existing double difference programs because it has potential advantages in model identification and covariance estimation. It was therefore of interest to compare this approach to the existing ones using a common data set.

### 1.1 Objectives and Outline of the Thesis

The original version of ASTRO was developed and tested using simulated GPS orbital information and phase data

(Wanless, 1985). The objective of this thesis is to use the ASTRO program package with observed GPS data to improve the existing single difference model and to determine whether the use of single differences is a viable approach to precise GPS positioning.

Single differences will contain more information about the orbital variations and the receiver clock errors than the double difference observations more commonly in use. Since orbital errors are one of the major limiting factors in precise GPS positioning (Beutler et al., 1987a), developing a workable single difference processing scheme could improve the overall positioning accuracy of the system.

A data set, observed with TRIMBLE 4000SX receivers on a set of well determined control points, was obtained from the Canadian Geodetic Survey (CGS). The test network and data set is discussed in section 1.2. To use this data set, The University of Calgary GPS data preprocessing package was modified to handle the data from all five observed satellites (see section 1.3). A number of other improvements to the ASTRO program were required to make it run with observed data. The major ones are the development of a method of computing the six initial Keplerian elements from the broadcast ephemeris parameters and the improvement of

bias modelling in the adjustment package, in particular, the modelling of receiver clock errors. The model and its improvements plus an analysis of the achieved results are discussed in this thesis.

A discussion of the mathematical formulation used in the adjustment and in the orbit prediction and improvement routines of the ASTRO program package is presented in Chapter 2. The observation equations and a brief review of the effects of improperly modelled biases is also presented.

The derivation of the method of computing the Keplerian initial conditions from the broadcast ephemeris is presented in Chapter 3. The satellite positions are determined for use in the adjustment package by integrating the equations of motion subject to the Keplerian initial conditions. A comparison of these satellite positions with those obtained directly from the broadcast ephemeris algorithm is presented.

Prior to implementing modifications of the original bias models, a number of adjustments were performed to assess the performance of the adjustment package. Results of these adjustments are presented in Chapter 4. Analysis of the results yields a number of alternative methods of revising the bias modelling, especially the clock model.

Results obtained from adjustments with the bias modelling changes implemented are presented in Chapter 5. Results of double difference adjustments, formulated to be compatible with ASTRO, plus the usual double difference formulation are introduced in Chapter 6. An analysis of the results along with recommendations for further research is presented in Chapter 7.

### 1.2 Layout of the Test Network

The data used for this analysis is a subset of the data used by the Geodetic Survey of Canada to evaluate the performance of the TRIMBLE 4000SX receivers and the TRIMVEC double difference GPS data processing program package. Baselines determined with the TRIMBLE/TRIMVEC system are accurate to within a few parts per million. The results of the complete test are presented in McArthur (1987).

The subset of the data, which is used for this study, consists of single frequency phase observations at three stations on November 14, 1986. The layout of the network is shown in Figure 1.1. The bulk of the analysis is performed on the baseline from station ROOF to station CATA.

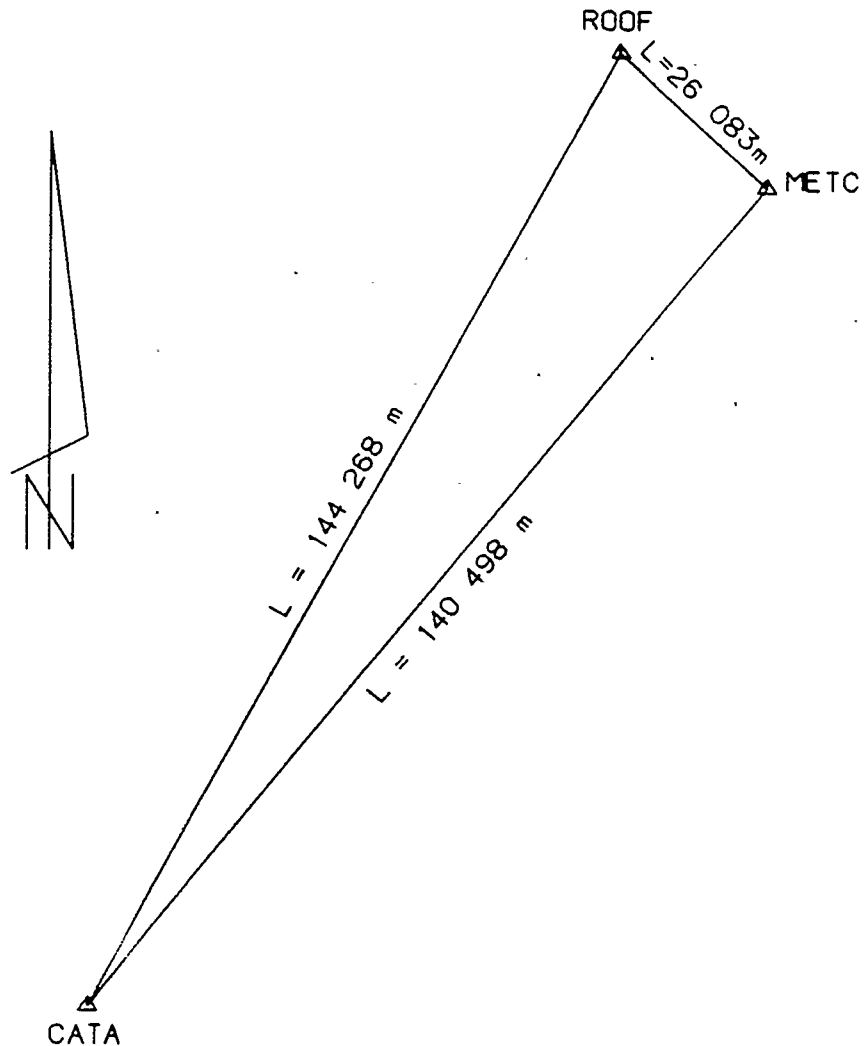


Figure 1.1: Layout of the Test Network

The data for baseline ROOF to CATA spans 4800 seconds, beginning at 488040 seconds from the Saturday midnight reference epoch of the broadcast ephemeris (about 11:00 AM local time). During the first 1000 seconds, five satellites were available while for the next 3600 seconds only four satellites were visible. The remaining 200 seconds of data has observations to only three satellites. A plot of the

GDOP values throughout the observation session is shown in Figure 1.2.

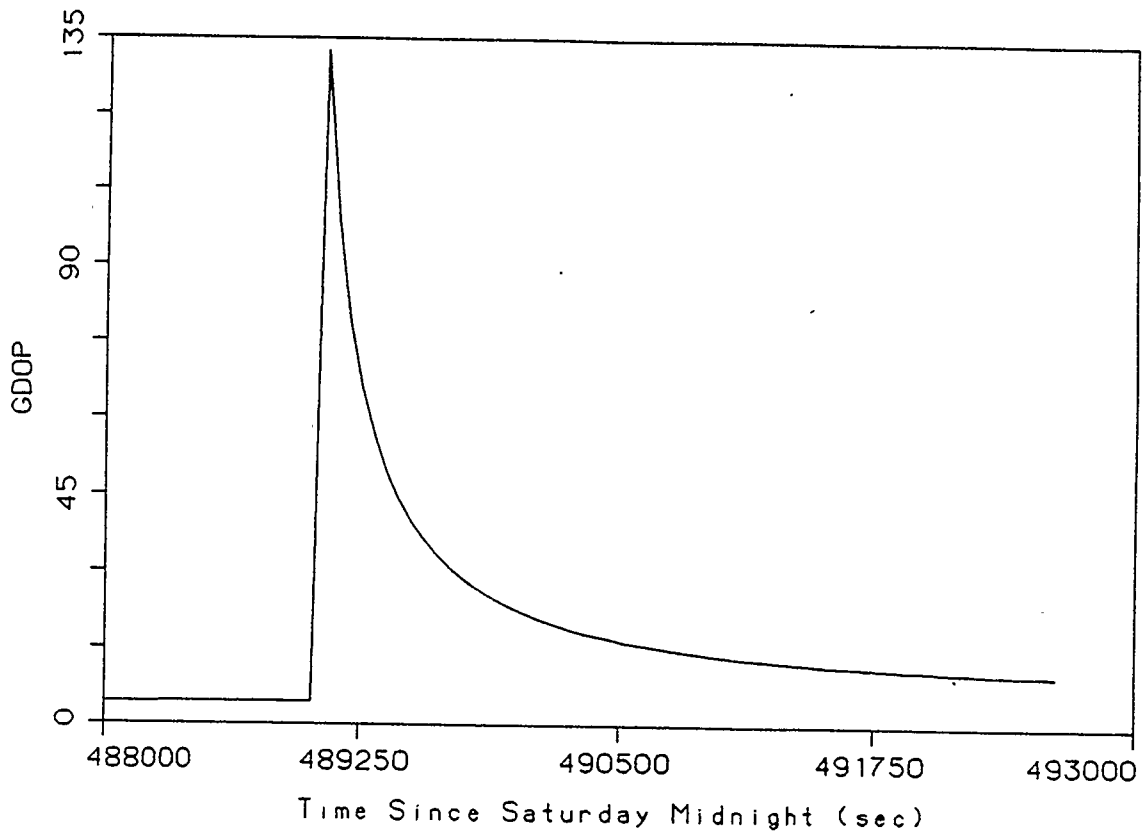


Figure 1.2: GDOP Throughout the Observation Session

Due to variations in the tracking start and stop times at each receiver, the other two baselines exhibit slightly different data spans. Both baselines ROOF to METC and METC to CATA start 450 seconds later. This reduces the five satellite coverage on METC to CATA to 550 seconds. The five satellite coverage on the baseline ROOF to METC lasts 400

seconds longer, thus removing the worst of the peak in the GDOP curve.

### 1.3 Data Preprocessor and Cycle Slip Correction Programs

The basic function of the preprocessor program is to correct cycle slips, identify and remove poor sections of data and produce the input files for use in the ASTRO program package. A Data Flow Diagram of the process is shown in Figure 1.3.

The raw data from the receiver is first converted to ASCII format and transferred to the mainframe computer. Cycle slip detection and correction is then performed on the raw observation files. Manual editing of poor sections of data is also performed at this step.

The cycle slip detection and correction routines are based on the method of Hilla (1986), slightly modified to handle the TRIMBLE 4000SX measurements (Tziavos, 1987). The entire algorithm can be divided into two main parts. In the first part, the larger cycle slips are identified with an algorithm which compares predicted and observed second differences of the carrier phase. In the second section, examination of first differences formed from the residuals

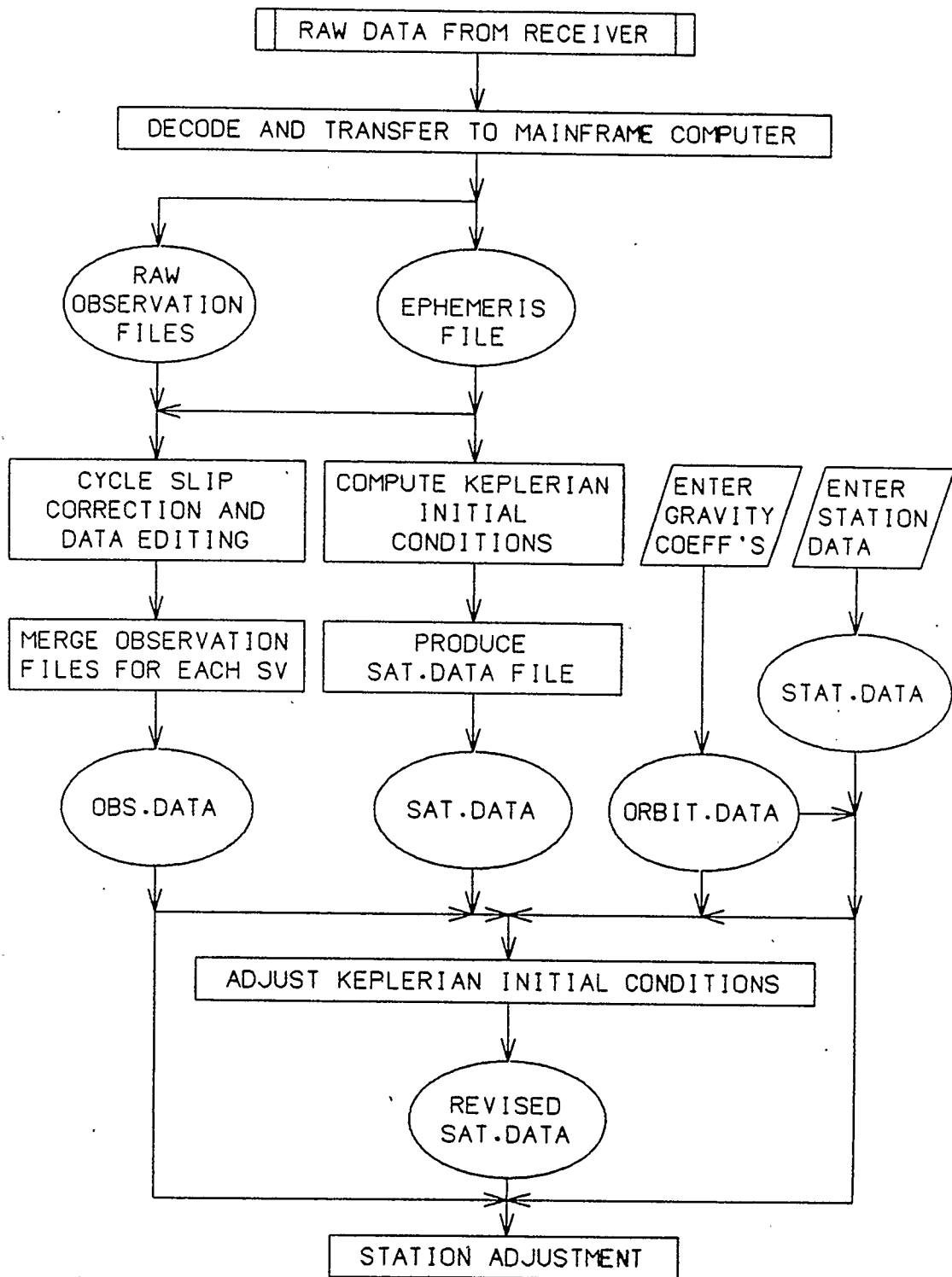


Figure 1.3: Preprocessor Data Flow Diagram

of a double difference adjustment identifies the remaining smaller cycle slips. A flowchart of the process is presented in Figure 1.4.

A first difference is defined as

$$\text{FDIFF}_j = P_j - P_{j-1} , \quad (1.1)$$

where  $P_k$  is the residual or carrier phase at epoch  $k$ , either predicted or observed. A second difference is defined as

$$\begin{aligned} \text{SDIFF}_{j+1} &= \text{FDIFF}_{j+1} - \text{FDIFF}_j , \\ \text{SDIFF}_{j+1} &= P_{j+1} - 2P_j + P_{j-1} . \end{aligned} \quad (1.2)$$

In the first part of the algorithm, the second differences of the predicted and observed carrier phases are compared by computing the delta second difference

$$\text{DSD} = \text{SDIFF}^P - \text{SDIFF}^O , \quad (1.3)$$

where  $\text{SDIFF}^P$  is the second difference formed from the predicted phase measurements and  $\text{SDIFF}^O$  is formed from the observed phase measurements. The predicted phase measurement is determined from the range based on the estimated position of the observing station and the satellite position computed from the broadcast ephemeris.

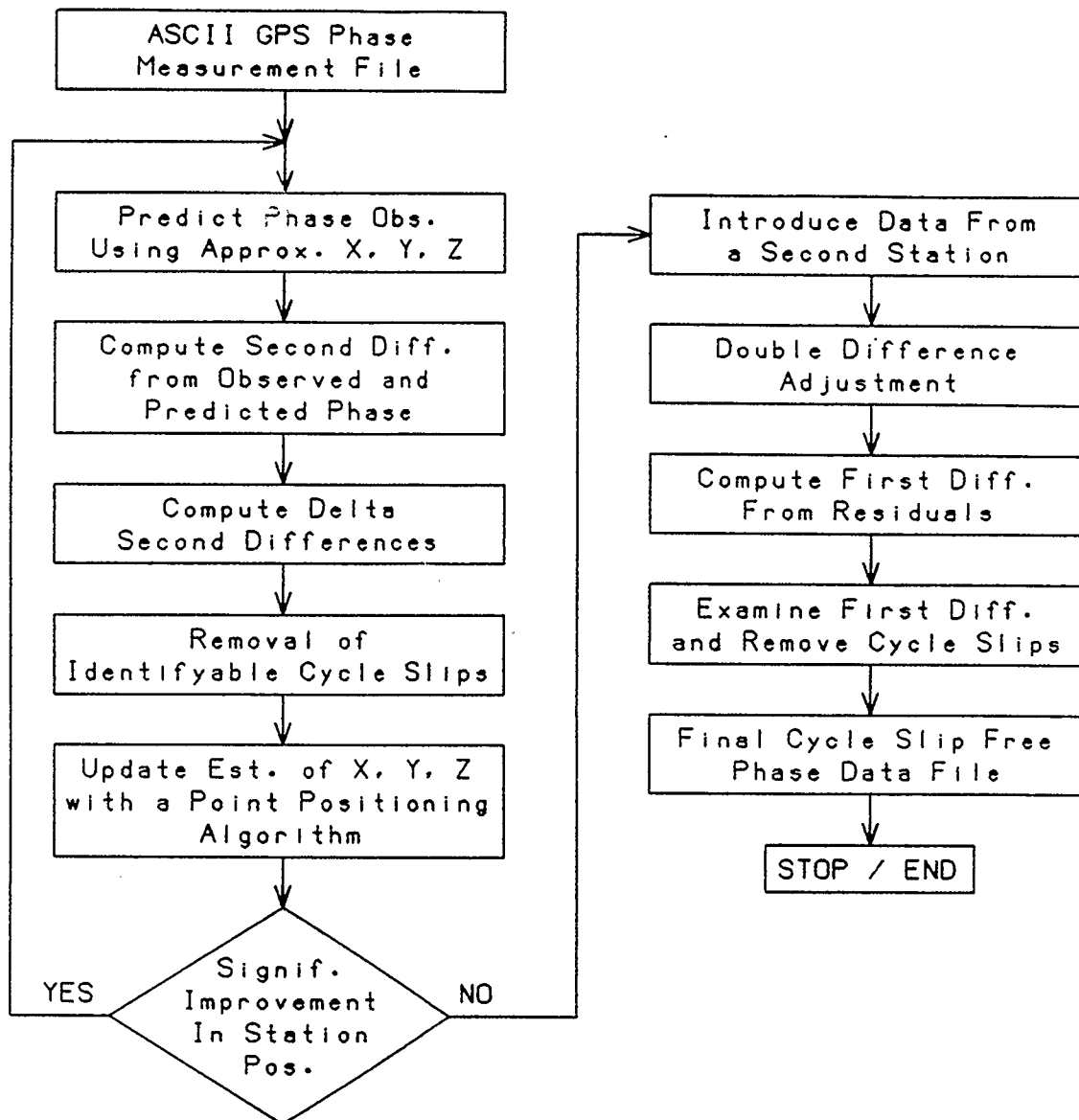


Figure 1.4: Cycle Slip Removal Flow Chart

The location of a cycle slip is identified when the DSD exceeds a certain tolerance level. The magnitude of the tolerance level is dependent on the accuracy of the estimated position of the observing station. The initial estimate of the station position needs only to be known to within ten kilometres. Once the larger cycle slips are removed, a point positioning algorithm is used to improve the estimate of the station position. This process is iterated until no further significant improvement is achieved in the station position. At this time, cycle slips greater than about five cycles will have been removed.

The remaining smaller cycle slips are corrected in the second stage. Data from a second station is introduced and a double difference adjustment is performed. Forming the first differences from the adjustment residuals shows the location of the remaining cycle slips. The first differences will be under one cycle if no cycle slip is present. A first difference greater than one cycle indicates a cycle slip of the same magnitude. These cycle slips are corrected and the final, clean phase data files are formed. The adjustment residuals may show further small cycle slips which can be removed from the data files at that time.

In the data from the test network, all observations with a large number of cycle slips at the beginning or end

of the data files were deleted. Between stations single difference phase observation files were then prepared from the cleaned phase observations of each satellite pass. The separate observation files are then combined to provide the final observation file for use in the ASTRO program package.

The current formulation of ASTRO requires that the satellite transmission times are identical for both of the one-way phase measurements that make up the single difference observation. In general, the signal transmit times only match to within one millisecond. The data are reduced to a common transmit time by interpolating the data at the free station end of the baseline, using the recorded phase velocity and time difference. All data which exhibited a transmit time difference of greater than one millisecond was deleted from the observation files.

The other input files shown in Figure 1.3 are entered manually. The station data file contains the initial station coordinates and clock coefficients. The gravity data file contains the harmonic coefficients of the gravity field,  $C_{l,m}$  and  $S_{l,m}$ . The process of determining the Keplerian initial conditions for use in the ASTRO program package is described in Chapter 3.

## CHAPTER 2

### BIAS MODELLING

Only a brief overview of the mathematical formulation used in ASTRO will be presented in this section. A complete discussion of the adjustment equations plus the orbit modelling techniques used in the original version of ASTRO can be found in Buffett (1985), Nakiboglu et al. (1985), and Wanless (1985). A review of the phase observation equations, receiver clock errors and atmospheric bias modelling used in ASTRO and other GPS data processing packages is also presented in this chapter.

The approach to GPS positioning used in ASTRO is to treat all of the data from a network of observing stations together in one solution for station position, nuisance parameters and orbit improvement. The choice of observable, for this study, is the between receiver single difference phase measurement. The single difference observable allows common biases such as receiver clock errors plus the remaining orbit errors and atmospheric propagation errors to be explicitly modelled. The price to be paid for explicitly modelling the biases is the large number of nuisance

parameters that must be solved for. The danger of overparameterizing the solution is therefore always present.

In the double and triple difference approaches, the common biases are cancelled. The higher differenced observables are used in several current GPS data processing program packages such as DIPOP (Vanicek, et al., 1985), NOVAS (Wanless and Lachapelle, 1988) and the Bernese Software (Beutler et al., 1987a), all of which have been very successful. Their main shortcoming is the insensitivity of double differences to the remaining systematic errors in the observations.

### 2.1 A Review of the Phase Observation Equations

Detailed discussions of the GPS phase observation equations can be found in the literature on the subject, see e.g. Remondi, 1984; Wei, 1986; Wells et al., 1986. The development of the equations will not be discussed here. Only a short overview, following the treatment of Wells et al. (1986) will be presented.

The one-way phase observation equation is

$$\Phi = \rho + c(dt - dT) + \lambda N - d_{\text{ion}} + d_{\text{trop}} , \quad (2.1)$$

where  $\Phi$  is the carrier beat phase measurement in length units,  $\rho$  is the range,  $c$  is the speed of light,  $dt$  and  $dT$  are the clock offsets from GPS time for the satellite and receiver respectively,  $\lambda$  is the carrier wavelength,  $N$  is the unknown ambiguity term,  $d_{ion}$  and  $d_{trop}$  are the ionospheric and tropospheric delays, respectively. Measurement noise, inherent in all observations, is not shown in equation (2.1).

The between receiver single difference (SD) observation equation is obtained by subtracting measurements from two receivers to the same satellite at identical epochs, i.e.

$$\Delta\Phi = \Delta\rho - c\Delta dT + \lambda\Delta N - \Delta d_{ion} + \Delta d_{trop}. \quad (2.2)$$

This observable greatly reduces the effects of satellite clock errors. Orbital and atmospheric errors are also reduced for baselines that are short in comparison to the altitude of the satellite.

The satellite clock error is only completely removed if the signal transmit time is identical for both carrier phase measurements. This is the approach adopted in the ASTRO program package. Only one satellite position is computed at each observation epoch; therefore both one-way phase measurements must be reduced at the same transmission time. This model allows more efficient use of the orbit

improvement facilities. The effects of this model formulation are further discussed in section 2.2.

An approach taken in other single difference processing packages, e.g. Remondi (1984), is to formulate the problem on the basis of the observations being quasi-simultaneous at the received time. A term describing the change in the satellite clock error over the difference in transmit times should now appear in equation (2.2). In view of the stability of the cesium clocks used on the satellites, this term can be considered negligible (Delikaraoglou, 1987).

In equation (2.2) the differenced receiver clock offset ( $\Delta dT$ ) is often solved for at each observation epoch unless further modelling is implemented, e.g. see Wei (1985); Remondi (1984). The clock offsets are modelled in the ASTRO program package with two second-order polynomials. The differenced cycle ambiguity term  $\Delta N$  is constant throughout the observation session, provided cycle slips do not occur. Wei (1985) has found it necessary to fix the receiver clock offset at the first observation epoch to avoid the singularity problem caused by very high correlations between the receiver clock offset and the ambiguities.

The receiver-satellite double difference (DD) observation equation, as shown below, is determined by

subtracting two simultaneous single differences, each to a different satellite; namely:

$$\Delta\nabla\Phi = \Delta\nabla\rho + \lambda\Delta\nabla N - \Delta\nabla d_{\text{ion}} + \Delta\nabla d_{\text{trop}} . \quad (2.5)$$

In addition to the errors removed by SD, DD also significantly reduces errors resulting from the differences between the two receiver clock offsets. Lindlohr and Wells (1985) have shown that these receiver specific biases are much more significant than the satellite specific biases. This feature is the main reason for the popularity of DD as the basic observable in GPS phase data processing software.

The receiver clock terms are only completely removed if all four one-way phase observations have identical received times. This will not normally be the case but the effects of the remaining receiver clock errors are reduced by a factor of  $10^5$  as compared to single differences. Even for precision applications, a linear clock model has proved sufficient for double difference observations (Beutler et al., 1987a).

## 2.2 Receiver Clock Modelling

GPS tracking data is based on the one-way signal travel-time. Therefore, errors due to the receiver and satellite clocks are inherent to the measurements. The carrier phase observations must be obtained simultaneously

because one of the most important sources of error results from fluctuations of the satellite and receiver reference oscillators. Forming differenced observations, or equivalently, modelling the variations greatly reduces the effects of the oscillator instabilities (Bock et al., 1986b). The degree by which the observations are not simultaneous will affect the ability to remove the errors.

The stability of an oscillator is usually described by the Allan variance or two sample variance. The Allan variance is a measure of the scatter of the second time derivative of a process (Skrumeda and Stephens, 1987). High quality quartz oscillators, used in most receivers, typically exhibit Allan variances of  $5 \times 10^{-12}$  over time spans of one second, increasing to  $10^{-11}$  at one hundred seconds (see Brown and Sturza, 1985; Clynch and Coco, 1986). The Allan variance of the cesium clocks used on board the GPS satellites is about  $10^{-12}$  at 100 seconds, decreasing to  $10^{-13}$  at  $10^5$  seconds (Swift, 1985).

The nondeterministic behaviour of the oscillator, as described by the Allan variance, has two effects on the phase measurements. First, the receiver reference phase will be in error since it is derived from the receiver oscillator. Second, the instabilities result in errors in the measurement time tags. The time tag errors are smaller

and can only be removed by modelling. The receiver reference phase error can be removed by modelling or by forming double differences (Clynch and Coco, 1986). The magnitude of the oscillator errors is independent of the distance between the observing stations (Bock et al., 1986b).

The ASTRO program package is based on a simultaneous transmit time model. The difficulty that arises from this formulation is that the two receiver clock offsets that are differenced to form the ASTRO SD are not measured at the same epoch. The differenced receiver clock offset term  $DdT$  will now contain a systematic component due to changes in the difference between the received times of the two signals. The clock offset term in equation (2.2) should now be written

$$\Delta dT = dT^2(T_2) - dT^1(T_1) , \quad (2.3)$$

where  $dT^2(T_2)$  is the second receiver's clock offset at epoch  $T_2$  and  $dT^1(T_1)$  is the first receiver's clock offset at epoch  $T_1$ . The magnitude of the systematic component will vary with changes in the satellite geometry with respect to the orientation of the baseline. The effect will reach a maximum when the observed satellite has traversed from horizon to horizon with rise and set points directly in line with the orientation of the baseline. The actual magnitude of the effect will be smoothly changing and is dependant on

baseline length. The effect can be reduced by modelling the receiver clock offsets by a polynomial, solving for them as a discrete white noise process or reducing the offsets to a common epoch by rewriting equation (2.3) as shown below

$$\begin{aligned}\Delta dT &= dT^2(T_2) - dT^1(T_2) - \delta dT^1, \\ \Delta dT &= \Delta dT - \delta dT^1,\end{aligned}\tag{2.4}$$

where  $\delta dT^1$  is the difference in the first receivers clock offset from epoch  $T_1$  to  $T_2$ . This clock drift can be obtained by fitting a first order polynomial to the receiver clock offsets determined from a pseudorange solution.

The data set output by the TRIMBLE receivers contains the clock offsets as derived from the pseudorange solution. The drift of the receiver clock at station CATA, determined from this data, is -0.021 cycles per second. Since the difference between the two received times is under one millisecond, the  $\delta dT^1$  correction will be a maximum of  $2.1 \times 10^{-5}$  cycles. The correction is less than the measurement noise, therefore it has been neglected.

The most common method of removing the clock biases is through forming double difference observations. For SD observations, a separate receiver clock bias is often solved for at each measurement epoch. This is equivalent to clock modelling by a discrete white noise process. The ability of

this method to properly resolve each clock bias is strongly dependent on satellite geometry (Delikaraoglou, 1987).

In order to increase the degrees of freedom in a single difference adjustment, a quadratic polynomial clock model is sometimes assumed. This is the approach adopted in the original version of ASTRO. A quadratic polynomial has proven adequate for modelling the residual clock bias effects for a double difference adjustment (Beutler, et al., 1987a) or where a very stable oscillator such as a cesium clock is used to supplement the receiver oscillator. A simple polynomial is generally not adequate for describing the behaviour of a quartz oscillator (see Remondi, 1984; Lindlohr and Wells, 1985).

The original ASTRO receiver clock model attempts to split the total clock errors into two equal components, each modelling one of the receiver clocks. The two polynomials are computed as follows:

$$\begin{aligned}\Delta dT^1 &= A_{01} f_1 + A_{11} f_1 (t-t_0) + A_{21} f_1 (t-t_0)^2, \\ \Delta dT^2 &= -A_{02} f_1 - A_{12} f_1 (t-t_0) - A_{22} f_1 (t-t_0)^2,\end{aligned}\tag{2.6}$$

where  $A_{ij}$  is the  $i$ -th order polynomial coefficient at the  $j$ -th station. The  $L_1$  carrier frequency is represented by  $f_1$ ,  $t$  is the observation epoch and  $t_0$  is the initial epoch.

The two clock polynomials in equations (2.6) are differenced while forming the misclosures, thus modelling the entire receiver clock offset as, effectively, a single polynomial. The problem with this type of formulation is that the corresponding clock coefficients will be linearly dependent; see Chapter 5 for details. The two receiver clocks are separate instruments, therefore, there should be no physical reason for this dependence.

The simple polynomial clock model does not account for time-tag errors in the measurements. This effect can be compensated for by adopting the single difference formulation given in Remondi (1984).

$$\begin{aligned} \Delta\Phi &= \Delta\rho + \{\dot{\rho}_2 - \dot{\rho}_1 + (f_{R2} - f_{R1})\lambda\}x_i - \{c - (\dot{\rho}_2 + \dot{\rho}_1)/2\}d_i \\ &\quad + \lambda\Delta N - \Delta d_{ion} + \Delta d_{trop} . \end{aligned} \quad (2.7)$$

Here, the clock error has been split into a common clock error,  $x_i$ , and a clock difference,  $d_i$ . The rate of change of the range is  $\dot{\rho}_i$  while  $f_{R2}$  and  $f_{R1}$  are the frequencies of the receiver oscillators. The term  $f_{R2} - f_{R1}$  can be determined from the relative clock drift computed from the pseudorange clock offsets logged in the data set.

The receiver oscillators normally agree to within 3 Hz and  $x_i$  is less than one millisecond (Remondi, 1984). Therefore, the term with the receiver clock frequencies is

negligible. The difference between the range rates is approximately one Hz per kilometre of baseline length (Remondi, 1984), therefore, this term is negligible for short baselines. Baselines less than 30 kilometres will produce errors less than the measurement noise. The range rate has a maximum value of  $800 \text{ m s}^{-1}$ . Since the receiver clock difference can be several milliseconds the term with the sum of the range rates can not be considered negligible.

Results of the adjustments performed with the full clock model given by equation (2.7) are presented in Chapter 5. In the new formulation, the two clock terms are modelled by separate second-order polynomials. In view of the different coefficients, the polynomials will no longer be completely linearly dependent.

Solving for clock biases as a white noise process disregards the fact that the biases are correlated from one epoch to another. By estimating the clock biases as a stochastic process, the correlations can be exploited and the time varying behaviour accounted for (Skrumeda and Stephens, 1987). Jones and Tryon (1987) have shown that the cesium clocks on the GPS satellites are well modelled by the sum of a random walk plus an integrated random walk process. A random walk process can adequately describe the behaviour of a cesium, rubidium or hydrogen maser. Random walk and

Gauss-Markov processes have not been successfully used for describing the behaviour of a quartz oscillator. Only a discrete white noise process has provided adequate results (Skrumeda and Stephens, 1987).

### 2.3 Atmospheric Propagation Delay Modelling

The atmospheric propagation delays are eliminated in the ASTRO program package by applying the corrections directly to the observations themselves. The tropospheric delay is modelled by applying the Hopfield Model (Hopfield, 1971). A scale factor to account for unmodelled tropospheric refraction is also solved for in the estimation model as discussed in section 2.4. The ionospheric delay model available in the GPS broadcast message is applied to each observation during the preprocessing stage.

The tropospheric delay is composed of a wet and a dry component, with the dry component accounting for about 90% of the total correction (Tralli, et al., 1988). The Hopfield Model is capable of removing 95 to 98% of the effect of the dry component (Remondi, 1984). The wet component is much less uniform and cannot be determined accurately from surface meteorological measurements. Beutler et al. (1987b) have shown that errors in the tropospheric correction for single differences result in a height bias plus a baseline

scale error. The height bias is independent of the baseline length, hence the relative error decreases as the baseline length increases. The tropospheric delay induced scale error is given a maximum value of 0.1 ppm, resulting in measured baseline lengths greater than the true length. Experimental results obtained by Tralli et al. (1988) indicate that simple atmospheric models result in baseline errors of up to 0.4 ppm in humid areas. The baseline error is reduced to a maximum of 0.1 ppm when a stochastic component is added to the tropospheric model and to about 0.08 ppm when WVR data is used to calibrate the tropospheric delay.

The ionospheric delay correction given in the broadcast message accounts for only about 50% of the actual delay (Klobuchar, 1982). Kleusberg (1986) computed the single difference of the ionospheric delays for a 40 km baseline and found high frequency noise at the one centimeter level plus a total variation of 20 cm over the two hours of data. The undifferenced data showed a total variation of 2.5 m. During a solar activity maximum, the total variation may approach 10 m with a similar increase in the high frequency noise (Campbell et al. 1986). Signals from satellites, observed at stations separated by more than 100 km, will generally pass through different and uncorrelated sections of the atmosphere yielding greater errors in the differenced delay (Delikaraoglou, 1987).

The effect of incorrectly modelling the ionospheric delay is to shorten the computed baseline length resulting in a scale error. Beutler et al. (1987b) have shown that the scale factor will be between 0.35 and 3.5 ppm for  $L_1$  observations, depending on the ion content of the atmosphere. Experimental results of Georgiadou and Kleusberg (1988) show a scale error that varies from 0.4 ppm to 0.7 ppm for fixed ambiguity, double difference solutions for baselines of 10 to 30 km. If ambiguities are solved for in the adjustment, a scale error of 0 ppm to 0.6 ppm results. The authors comment that the difference between the results is due to the unknown ambiguities absorbing a portion of the ionospheric delay.

The effects of the ionospheric delay can be further reduced for single frequency GPS users by incorporating a more descriptive model see e.g. Campbell et al. 1986; Georgiadou and Kleusberg, 1988. Unfortunately, these methods require additional information from nearby dual frequency monitoring stations which was not available for the data set used in this study.

#### 2.4 ASTRO Adjustment Software

The estimation model used in ASTRO consists of two implicit models,  $f_1$  and  $f_2$ , namely (Wanless, 1985):

$$\begin{aligned} f_1(X, X', l) &= 0 ; C_x, C_l, \text{ and} & (2.8) \\ f_2(X', Z_0) &= 0 ; C_{Z_0}, \end{aligned}$$

where  $X$  is the vector of ground station Cartesian coordinates,  $X'$  are the satellite coordinates and solar radiation pressure scale factor,  $Z_0$  are the six initial state Keplerian elements ( $a, e, \omega, i, \Omega, M$ ) and  $l$  is the vector of observables. The vector  $X$  also includes nuisance parameters corresponding to:

- tropospheric refraction scale factor,
- cycle ambiguities,
- second order polynomial coefficients to model receiver clock biases.

The satellite position is determined by integrating the equations of motion, subject to the six initial state Keplerian elements.

The function  $f_1$  is a pure geometric mode model while  $f_2$ , the orbit improvement model, is defined from a force model relating the satellite initial conditions and the satellite position coordinates at an arbitrary epoch. That is,  $f_2$  is the solution of the equations of motion in terms of the initial conditions.

The linearized form of the function  $f_1$  is

$$A_x \delta X + A_{x'} \delta X' + w = r, \quad (2.9)$$

where  $A_x$  and  $A_{x'}$  are the design matrices,  $w$  is the misclosure vector,  $\delta X$ ,  $\delta X'$  and  $r$  are corrections to the unknowns and observations respectively. The linearized form of the second model  $f_2$  is

$$X' = BZ_0, \quad (2.10)$$

or in differential form

$$\delta X' = B \delta Z_0, \quad (2.11)$$

where

$$B = B_1 B_2, \quad (2.12)$$

$$B_1 = \frac{\delta X'(t)}{\delta Z(t)}, \quad B_2 = \frac{\delta Z(t)}{\delta Z_0}.$$

Equations (2.12) describe the variations of the Keplerian orbital elements resulting from the variations of the initial state vector  $\delta Z_0$ . The  $B_2$  matrix propagates  $\delta Z_0$  forward in time to the current observation epoch,  $t$ . The resulting changes in the osculating Keplerian elements  $\delta Z(t)$  are then propagated into the satellite Cartesian coordinates by the  $B_1$  matrix. Equation (2.12) is also used in the process to determine the value of the Keplerian initial state vector from the broadcast ephemeris as is discussed in

Chapter 3. The explicit form of the  $B_1$  and  $B_2$  matrices can be found in Buffett (1985) or Nakiboglu et al. (1985).

The forgoing method of accounting for the variation of the Keplerian orbital elements has been shown to be accurate and computationally efficient. Errors in the initial conditions of up to 200 metres can be propagated with a nonlinearity of under one metre for orbital arcs of up to four hours duration (Nakiboglu et al., 1985).

Substitution of equation (2.12) into (2.9) yields the estimation model used in ASTRO, namely:

$$A_x \delta X + A_x' B \delta Z_0 + w = r, \quad (2.13)$$

with a priori covariance information  $C_x$ ,  $C_{Z_0}$  and  $C_1$ . Using Equation (2.13), the estimation process has proven to be computationally efficient. On the first iteration, satellite coordinates are computed by integrating the equations of motion in terms of the six initial state Keplerian elements by Cowell's method (Conte, 1963). On subsequent iterations, orbit improvement is determined by analytical computations based on equations (2.11) and (2.12).

### CHAPTER 3

#### COMPUTATION OF THE KEPLERIAN INITIAL CONDITIONS FROM THE BROADCAST EPHEMERIS

As noted in previous chapters, the ASTRO program package was written to handle only simulated data. During the initial studies conducted by Buffett (1985) and Wanless (1985) the Keplerian initial conditions were established from specifications for the GPS constellation. To use the ASTRO program package with observed data, a method of estimating the Keplerian initial conditions from the broadcast ephemeris is required. The remainder of this chapter is devoted to discussing the broadcast ephemeris and the method of obtaining the Keplerian initial state vector.

The underlying reasons for determining the satellite positions by numerical integration rather than directly from the broadcast ephemeris are threefold. First, integrated orbits allow the use of orbit improvement techniques. Second, the orbit will be smoother. Since the broadcast ephemeris has only a one and a half hour period of applicability, longer observation sessions will require the use of two or more ephemeris blocks. A jump in the satellite

positions is common when changing from one block to another. Finally, the accuracy of the orbit can be tuned by varying the force model and a priori variances of the Keplerian initial conditions.

### 3.1 Review of the Broadcast Ephemeris

The current broadcast ephemeris can be in error by up to 50 metres (Delikaraoglou, 1987). A precise ephemeris is also being computed by the Naval Surface Weapons Centre. The accuracy of the precise ephemeris is not well known but an evaluation by Swift (1985) indicates errors of as much as 6, 43 and 25 metres in the radial, along-track and across-track directions respectively. When the operational constellation is in place, the accuracy of the broadcast ephemeris is expected to be of the order of 1.5 metres in the radial direction (Van Dierendonck et al., 1980). Wells, et al. (1986) indicate that the actual errors are more likely in the five metre range.

The broadcast ephemeris is readily available in the navigation message modulated on the GPS signal. The position of the satellite is defined by a set of parameters similar to Keplerian orbital elements, which describe a smooth elliptical orbit. There is also an additional set of

parameters which model perturbations about the elliptical orbit. The additional parameters primarily account for the effects of the non-sphericity of the earth plus smaller perturbations resulting from luni-solar gravitation and solar radiation pressure (King et al., 1985).

The broadcast ephemeris parameters are the result of a curve-fit extrapolated into the future. They are intended for use only in the one and a half hour period of applicability. They do not adequately describe the orbit perturbations over long periods of time (Van Dierendonck, 1980; King et al., 1985).

### 3.2 Method of Computing the Keplerian Initial Conditions

The algorithm to compute the earth centered/earth fixed Cartesian coordinates of the satellite from the broadcast ephemeris parameters can be found in several publications, for example Van Dierendonck (1980); King et al. (1985) or Wells et al., (1986). In addition, the three Cartesian velocities are required. These six parameters are then transformed into the six Keplerian initial conditions.

This subsection is devoted to first developing the equations to compute the satellite Cartesian velocities from

the broadcast ephemeris parameters. Next, the transformation from Cartesian to Keplerian orbital elements is discussed.

The Conventional Terrestrial (CT) System coordinates of the satellite at the  $k$ -th epoch,  $\mathbf{x}_k$ , are given by

$$\mathbf{x}_k = \mathbf{R}_3(-\lambda_k) \mathbf{R}_1(-i_k) \mathbf{R}_3(u_k) \mathbf{r}_k, \quad (3.1)$$

where  $\mathbf{R}_i$  are rotation matrices,  $\lambda_k$  is the longitude of the ascending node,  $i_k$  is the inclination,  $u_k$  is the argument of latitude and  $\mathbf{r}_k = [r_k \ 0 \ 0]^T$  is the orbital radius vector. The argument of latitude is the angular distance from the ascending node to the satellite position. The orbital radius vector is the vector from the geocentre to the satellite. The parameters in Equation (3.1) are computed from the existing broadcast ephemeris algorithm as shown below:

$$u_k = \omega + f_k + C_{uc} \cos[wf] + C_{us} \sin[wf], \quad (3.2)$$

$$r_k = a(1 - e \cos E_k) + C_{rc} \cos[wf] + C_{rs} \sin[wf], \quad (3.3)$$

$$i_k = i_o + \dot{i} t_k + C_{ic} \cos[wf] + C_{is} \sin[wf], \quad (3.4)$$

$$\lambda_k = \Omega_o + (\dot{\Omega} - \omega_e) t_k - \omega_e t_{oe}, \quad (3.5)$$

$$wf = 2(\omega + f_k), \quad (3.6)$$

where  $a$  is the semi-major axis and  $e$  the eccentricity of the orbit,  $E_k$  is the eccentric anomaly,  $\omega$  is the argument of perigee,  $f_k$  is the true anomaly,  $\Omega$  and  $\dot{\Omega}$  are the right ascension of the ascending node and its time derivative and  $\omega_e$  is the rotation rate of the earth. The coefficients  $C_{jc}$

and  $C_{js}$  are the amplitudes of the cosine and sine harmonic perturbations of the  $j$ -th element.

The Cartesian satellite velocities,  $\mathbf{x}_k$ , are obtained by differentiating equation (3.1) with respect to time

$$\begin{aligned} \dot{\mathbf{x}}_k &= - \frac{d\mathbf{R}_3(-\lambda_k)}{d\lambda_k} \frac{d\lambda_k}{dt} \mathbf{R}_1(-i_k) \mathbf{R}_3(-u_k) \mathbf{r}_k \\ &\quad - \mathbf{R}_3(-\lambda_k) \frac{d\mathbf{R}_1(-i_k)}{di_k} \frac{di_k}{dt} \mathbf{R}_3(-u_k) \mathbf{r}_k \\ &\quad - \mathbf{R}_3(-\lambda_k) \mathbf{R}_1(-i_k) \frac{d\mathbf{R}_3(-u_k)}{du_k} \frac{du_k}{dt} \mathbf{r}_k \\ &\quad + \mathbf{R}_3(-\lambda_k) \mathbf{R}_1(-i_k) \mathbf{R}_3(-u_k) \frac{d\mathbf{r}_k}{dt} \end{aligned} \quad (3.7)$$

where, by differentiating equations (3.2) to (3.6) with respect to time

$$d\lambda_k/dt = \dot{\Omega}, \text{ from the broadcast ephemeris,} \quad (3.8)$$

$$di_k/dt = \dot{i} + 2\dot{f}_k\{-C_{ic}\sin[wf] + C_{is}\cos[wf]\}, \quad (3.9)$$

$$du_k/dt = \dot{f}_k\{1 - 2C_{uc}\sin[wf] + 2C_{us}\cos[wf]\}, \quad (3.10)$$

$$d\mathbf{r}_k/dt = [ dr_k/dt \quad 0 \quad 0 ]^T, \quad (3.11)$$

$$dr_k/dt = ae\dot{E}_k\sin(E_k) - 2\dot{f}_k\{C_{rc}\sin[wf] + C_{rs}\cos[wf]\}. \quad (3.12)$$

The values of all parameters in Equations (3.2) to (3.12) are either given in the broadcast ephemeris or computed in the initial steps of the algorithm. The only exceptions are

$$\dot{E}_k = \frac{n}{1 - e \cos E_k}, \text{ and} \quad (3.13)$$

$$\dot{f}_k = \frac{n(1 + e \cos f_k)^2}{(1 - e^2)^{3/2}}, \quad (3.14)$$

where  $n$  is the mean motion and  $E_k$  is the eccentric anomaly. Equations (3.13) and (3.14) are derived from the equations for an unperturbed orbital ellipse (see Danby, 1962).

In equations (3.7) to (3.12), the effects of  $\dot{a}$ ,  $\dot{e}$ ,  $\dot{\omega}$  and  $\dot{\omega}_e$  and of the harmonic term time derivatives have been neglected. To evaluate the effects of this approximation, the long term perturbation of the orbit due to the most prominent force,  $C_{20}$  can be computed. They are

$$\begin{aligned} \dot{a} &= 0, & \dot{e} &= 0, & \dot{i} &= 0, \\ \dot{\omega} &= \frac{3 n C_{20} a_e^2}{4(1 - e^2)^2 a^2} (1 - 5 \cos^2 i) \end{aligned} \quad (3.15)$$

where  $a_e$  is the semi-major axis of the earth (Arden, 1987).

The magnitude of  $\dot{\omega}$  is approximately  $2 \times 10^{-10}$  rad  $s^{-1}$  which is negligible over the time frames considered. Superimposed on the long term perturbations are shorter term effects which can be significant over several hours (see Buffett, 1985). The change in the rotation rate of the earth also consists of a long term trend with shorter term effects

superimposed. The mean value of  $\dot{\omega}_e$ , given in Moritz and Mueller (1976) is  $-1.23 \text{ ms cy}^{-1}$ , which is clearly negligible. The shorter term effects have periods of a few days and longer, thus they can also be considered negligible.

The CT system coordinates and velocities are rotated into the inertial coordinate system used by the orbit prediction section of ASTRO (see Buffett, 1985) by

$$\mathbf{x} = \mathbf{R}_3(-\theta)\mathbf{X}, \quad (3.16)$$

where  $\mathbf{x}$  and  $\mathbf{X}$  are the inertial and CT system coordinates or velocities respectively and  $\theta$  is the Greenwich Apparent Sidereal Time (Wells, 1986).

The equations for the transformation of the inertial coordinates and velocities to the Keplerian elements describing the instantaneous orbital ellipse are given in Kaula (1966, pg 22-23). Note that these equations are developed from the equations for an unperturbed orbit. This algorithm exhibits a difficulty in separating  $\omega$  and  $M$  due to their similarity and the poor definition of the point of perigee for low eccentricity orbital ellipses.

### 3.3 Comparison of the Satellite coordinates from the Broadcast Ephemeris and the Estimated Initial Conditions

The orbit prediction section of the ASTRO program integrates the equations of motion subject to the Keplerian initial conditions to compute the satellite Cartesian coordinates in the inertial system. The inertial coordinates are then rotated into the CT system for use in the adjustment package.

Figure 3.1 shows the difference between the satellite positions computed from the broadcast ephemeris and those computed by the orbit integration section of the ASTRO program package, using the original estimate of the initial conditions. A summary of the mean coordinate and velocity differences for each of the observed satellites is presented in Table 3.1, denoted run 1. The estimate of the Keplerian initial conditions is presented in Tables 3.2 to 3.4 for each of the three satellites shown in Figure 3.1.

Figure 3.1 shows that the error in the satellite position grows in time to an unacceptable level indicating that the original estimate of the initial conditions is in error. These errors arise for several reasons. First, there are approximations used in deriving the equations for the satellite Cartesian velocities. Also, the broadcast

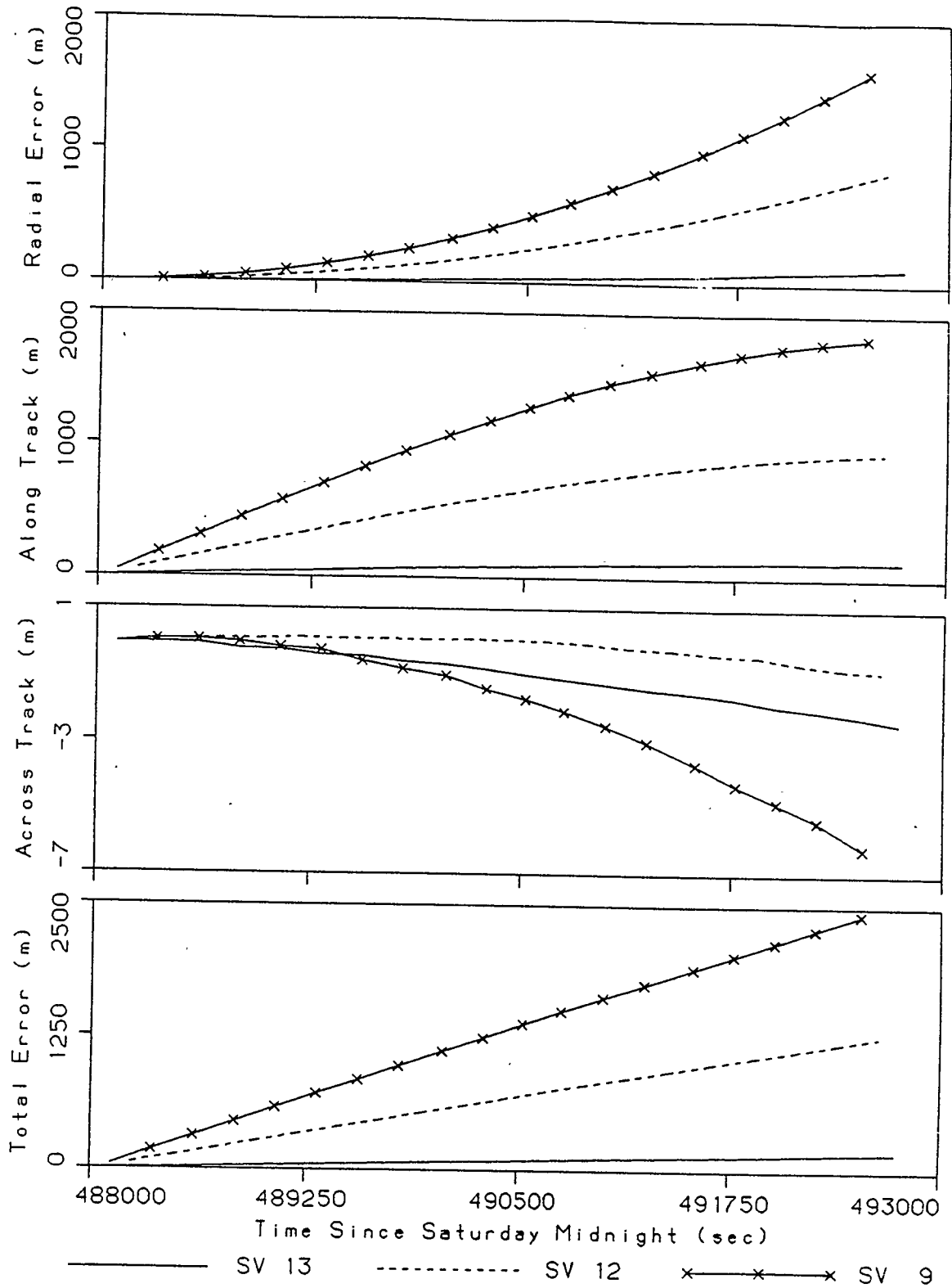


Figure 3.1: Satellite Position Errors; First Estimate

Table 3.1: Mean Coordinate and Velocity Differences

Sat. PRN	Run 1		Run 2		Run 3	
	Coord. Diff. (m)	Vel. Diff. (m/s)	Coord. Diff. (m)	Vel. Diff. (m/s)	Coord. Diff. (m)	Vel. Diff. (m/s)
Sat 13	91.89	0.016	3.39	0.040	0.24	0.040
Sat 12	679.55	0.120	53.67	0.290	0.84	0.290
Sat 11	1160.00	0.204	146.94	0.492	0.27	0.498
Sat 9	1273.50	0.225	172.63	0.570	0.93	0.562
Sat 6	39.71	0.004	9.79	0.076	0.10	0.076

Table 3.2: Estimates of the Keplerian Initial Conditions;  
Satellite PRN 13

Element	Run 1	Run 2	Run 3	Run 3-Run 1
a(m)	26560628.8	26561168.3	26561168.4	539.6
e(rad)	0.00316501	0.00317866	0.00317869	0.00001368
$\omega$ (rad)	-0.25142011	-0.24669206	-0.24670937	0.00471074
i(rad)	1.09289968	1.09289956	1.09289956	$-1.14 \times 10^{-7}$
$\Omega$ (rad)	2.24349483	2.24349474	2.24349473	$-9.8 \times 10^{-8}$
M(rad)	0.82124513	0.81651742	0.81653476	-0.00471037

Note: An angular change of  $10^{-5}$  rad corresponds to a displacement of 250 metres.

Table 3.3: Estimates of the Keplerian Initial Conditions;  
Satellite PRN 12

Element	Run 1	Run 2	Run 3	Run 3-Run 1
a (m)	26553936.8	26557866.6	26557879.7	3942.9
e (rad)	0.00890364	0.00876877	0.00876858	-0.00013506
$\omega$ (rad)	-1.01655128	-1.00936802	-1.00923340	0.00731788
i (rad)	1.10799321	1.10799323	1.10799323	$1.90 \times 10^{-8}$
$\Omega$ (rad)	0.13544303	0.13544297	0.13544297	$-5.9 \times 10^{-8}$
M (rad)	2.69738703	2.69020277	2.69006814	-0.00731889

Table 3.4: Estimates of the Keplerian Initial Conditions;  
Satellite PRN 9

Element	Run 1	Run 2	Run 3	Run 3-Run 1
a (m)	26553171.2	26560929.8	26560926.0	7754.8
e (rad)	0.01199147	0.01206013	0.01206344	0.00007197
$\omega$ (rad)	1.16225268	1.18587458	1.18571327	0.02346059
i (rad)	1.11667209	1.11667244	1.11667244	$3.42 \times 10^{-7}$
$\Omega$ (rad)	0.13091861	0.13091840	0.13091840	$-2.11 \times 10^{-7}$
M (rad)	1.31761920	1.29399791	1.29415907	-0.02346013

ephemeris parameters are a result of a curve-fit extrapolated into the future. They describe the satellite position over the one and a half hour period of applicability but they do not describe the entire orbit (Van Dierendonck, 1980).

A closer match between the satellite coordinates is obtained by performing an adjustment of the Keplerian initial conditions using the equations to propagate errors in the initial conditions over time. Combining equations (2.5) and (2.6)

$$\delta X' = B_1 B_2 \delta Z_0 , \quad (3.7)$$

where  $\delta X'$  is the vector of satellite coordinate errors,  $\delta Z_0$  is the error in the Keplerian initial conditions to be solved for, while  $B_1$  and  $B_2$  are the propagation matrices. The vector  $\delta X'$  has three elements for each epoch while the  $B_1 B_2$  matrix consists of a three by six block for each epoch.

A plot of the errors in the satellite positions, computed using the adjusted Keplerian initial conditions is presented in Figure 3.2, denoted as run 2. Most of the large drifts evident in Figure 3.1 have now been removed. The mean coordinate and velocity differences have been reduced, as shown in Table 3.1, although the difference is still too large. The estimate of the new Keplerian initial conditions is shown in Tables 3.2 to 3.4.

The remaining error in the satellite positions is a result of the modelling used to produce the  $B_2$  matrix. This matrix is based on linear perturbation theory using only the effects of  $C_{20}$  in the force model. This formulation allows

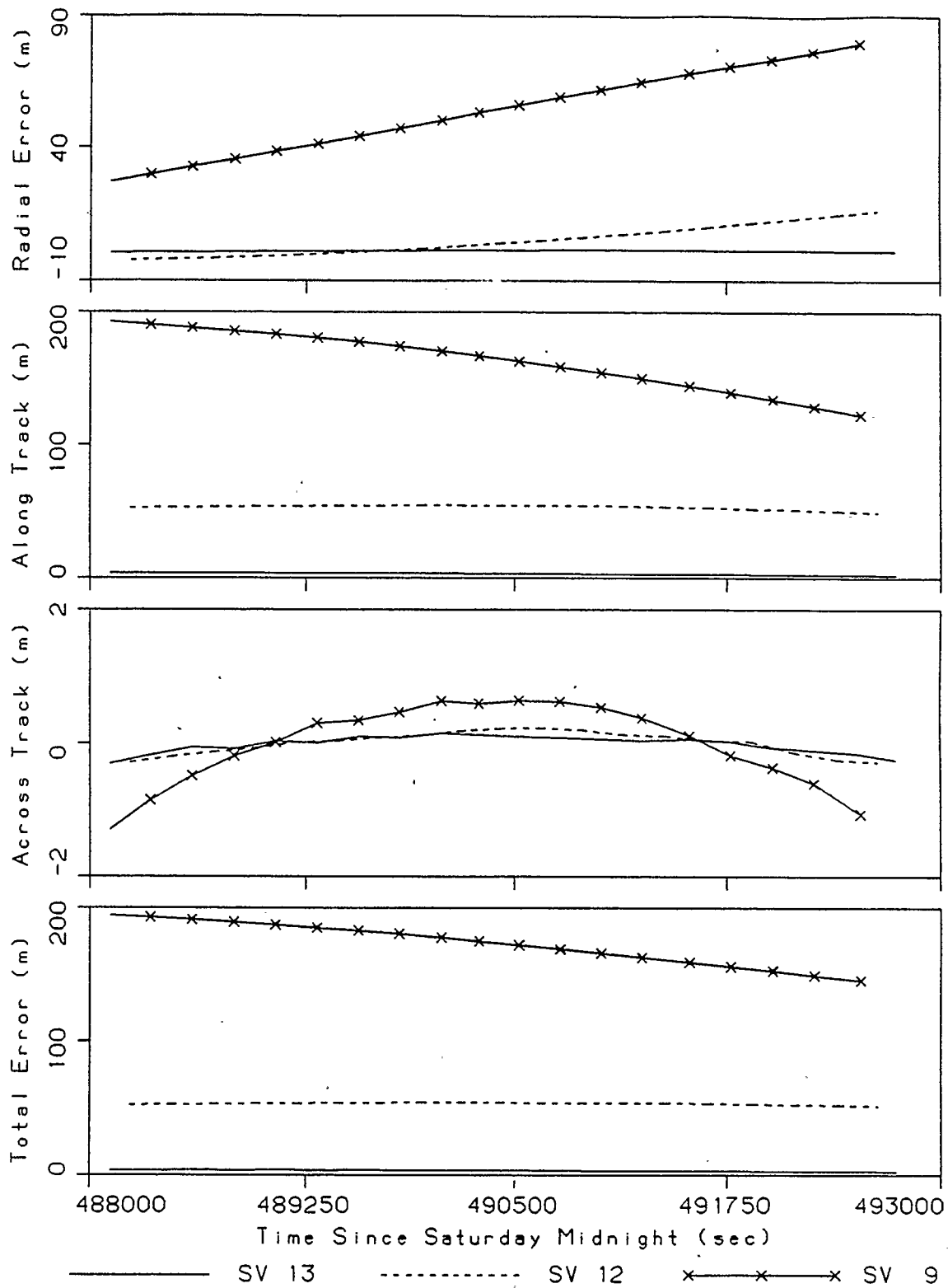


Figure 3.2: Satellite Position Errors; Second Estimate

errors in the initial conditions of approximately 200 metres to be propagated with a nonlinearity of under 1 metre for orbital arcs of up to 4 hours duration (Buffett, 1985; Nakiboglu et al., 1985). The errors in the original initial conditions exceeded 200 metres, hence, the  $B_2$  matrix does not properly model the required change.

To remove the remaining error, the adjustment is repeated using the second set of position differences, in the  $\delta X'$  vector. Recomputing the satellite positions with the third estimate of the Keplerian initial conditions yields the satellite position differences shown in Figure 3.3. The mean coordinate and velocity differences are presented in Table 3.1. The difference between the two sets of satellite positions are now under two metres, clearly acceptable given the accuracy of the broadcast ephemeris.

The final estimate of the Keplerian initial conditions is presented in Tables 3.2 to 3.4 along with the difference between the initial and final estimates. The primary changes are in the elements defining the size of the orbital ellipse,  $a$  and  $e$ , which was to be expected since the prediction was determined at a single point. Also note that the corrections to the argument of perigee,  $\omega$  and the mean anomaly  $M$  nearly cancel each other. As previously noted, the algorithm used to transform the satellite Cartesian

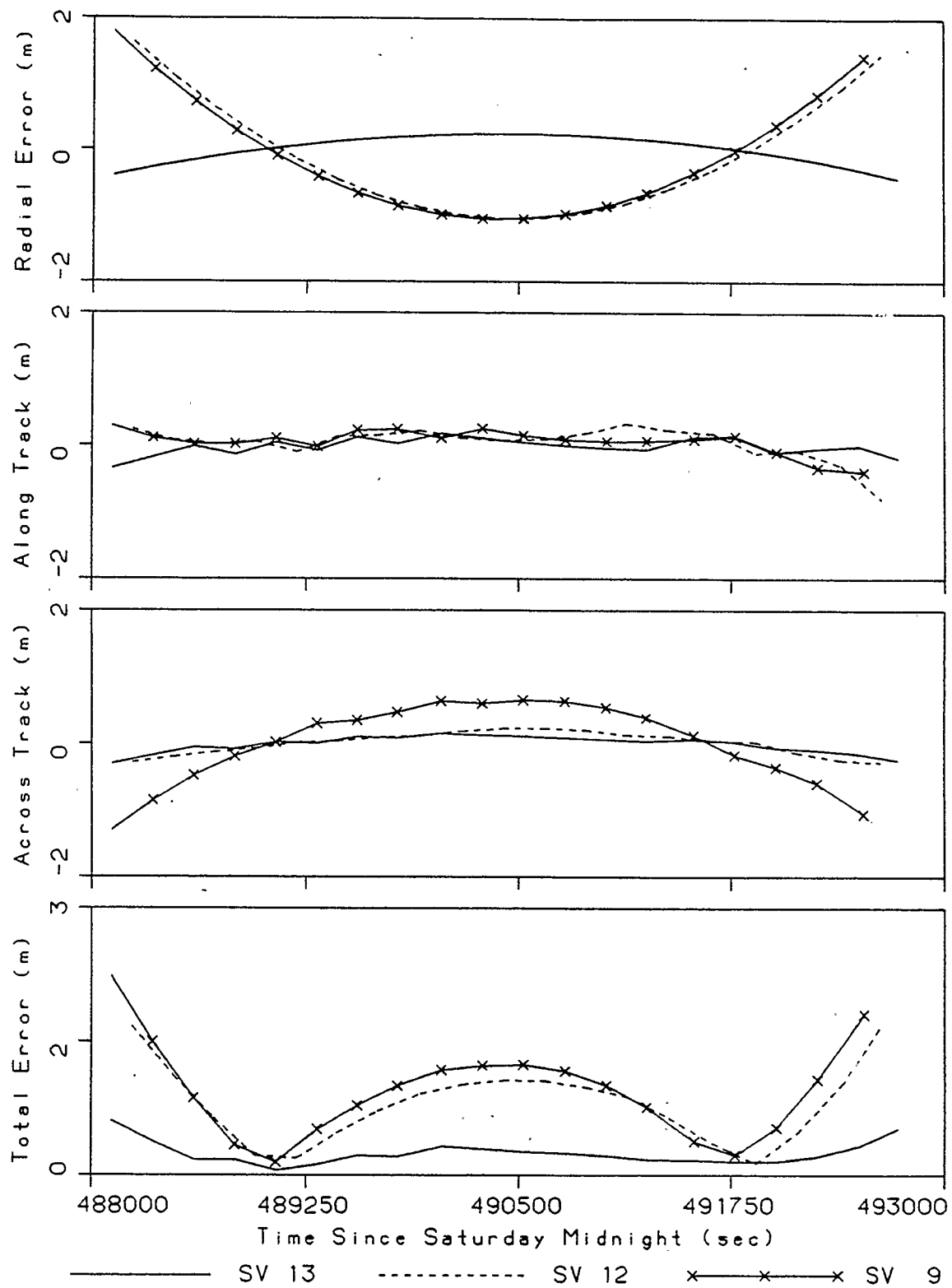


Figure 3.3: Satellite Position Errors; Final Estimate

coordinates and velocities into the Keplerian elements has difficulty separating these two components. The incorrect value of  $M$  contributed to the satellite position error growing in time, primarily in the along-track direction.

Comparing Figures 3.1 and 3.3 shows that the satellite position at the first epoch, where the initial conditions were predicted, has changed by less than two metres. This indicates that the original estimate represented the initial satellite position accurately but not the velocities. The final estimate of the initial conditions represents both the satellite position and the velocities more accurately.

The remaining systematic trend is a result of differences between the algorithms used to predict the orbit. Neglected effects in both orbit representations will also contribute to the systematic trend.

The ultimate accuracy of the satellite positions is now dependent upon the accuracy of the original ephemeris. This is important only if a single baseline is being processed since orbit improvement capabilities can then not be utilized. If data from a network of stations is being processed in one adjustment, the orbit improvement capabilities can be utilized and a further improvement of the orbit can be expected (see Wanless, 1985).

## CHAPTER 4

### POSITIONING 'RESULTS WITHOUT MODEL REFINEMENTS

This chapter presents the results of processing the test data with the original version of ASTRO without model refinements implemented. The analysis of these results points out a number of model weaknesses, thus laying the groundwork for implementing improvements to the bias modelling. The Keplerian initial conditions, determined in Chapter 3, were used to define the orbit. Each baseline was processed separately while holding the orbit fixed. To utilize ASTRO's orbit improvement capabilities, a minimum of three observing stations in a network with a spatial extent of a few hundred kilometres or more is required.

As noted in chapter 3, the orbit computed by ASTRO matches the broadcast ephemeris orbit to within two metres. The broadcast ephemeris itself may be in error by up to 50 metres hence some error is expected in the baseline computations. A conservative estimate of this effect can be determined from the rule of thumb given by Beutler et al., (1984).

$$\frac{dB}{B} = \frac{dr}{r}, \quad (4.1)$$

where B and dB are the baseline length and its corresponding error respectively, r is the average topocentric range to the satellite and dr is the orbit error. The rule of thumb implies that baseline errors of up to two ppm may result from satellite position errors in the broadcast ephemeris.

#### 4.1 Initial Results on All Baselines

The ASTRO program solves for the unknown station coordinates directly. The error in the computed station coordinates (computed minus GSC published values) for each baseline is given in Table 4.1. The numbers given in brackets are the errors in parts per million. Baseline ROOF to CATA is denoted run 4.1, ROOF to METC corresponds to run 4.2, while METC to CATA is denoted run 4.3. Appendix A also gives a brief description of each adjustment. Station ROOF is held fixed at the GSC published values in both baselines containing this station. Station METC is fixed in baseline METC to CATA. Unknown station coordinates are treated as weighted parameters with an a priori variance of 25 m<sup>2</sup> in each component. Published coordinates are entered as the initial estimate. Ambiguities were solved for as free parameters.

The variance applied to the station coordinates reflects a conservative estimate of the accuracy of the initial position. In a production survey situation, where the station coordinates are obtained from the double difference adjustment in the preprocessor, the variance will be lower. In the current study, the variance was kept high so as not to unduly influence the results.

Each receiver clock was modelled by separate second order polynomials as discussed in chapter 2. A value of zero was entered as the initial estimate of the coefficients. Although the a priori knowledge was limited to the assumption that the coefficients would be close to zero, a relatively low variance was used. Entering a higher variance resulted in singular normal equations. An observation variance of one metre<sup>2</sup> was also used to prevent singularities in the normal equations. The a posteriori variance factor for each of the adjustments was 1.134, 23.284 and 15.862 for runs 4.1 to 4.3 respectively, indicating modelling problems.

The results for runs 4.2 and 4.3, shown in Table 4.1, are clearly unacceptable. Atmospheric delay and orbital errors should contribute only a few parts per million to the baseline error, thus they can not be the major error source. Improper modelling of the receiver clock difference, poor

orbital geometry and instabilities in the adjustment equations are the remaining possible error sources.

Table 4.1: Baseline Errors from Initial Runs

Run Number	X	Errors in m and (ppm)			Length
		Y	Z	Pos.	
4.1	-0.380	-0.113	0.043	0.399	0.173
R-C	(8.4)	(1.1)	(0.5)	(2.8)	(1.2)
4.2	1.436	-3.189	-0.746	3.576	2.444
R-M	(65.9)	(437.)	(60.4)	(137.)	(93.7)
4.3	2.234	-2.700	0.859	3.608	0.304
M-C	(33.3)	(28.1)	(11.1)	(25.7)	(2.2)

The adjustment residuals from three of the satellites in each of runs 4.1 to 4.3 are shown in Figures 4.1 to 4.3. The similarity of the residual curves from each satellite further strengthens the assumption that the error arises from a receiver or baseline specific source such as the receiver clock model. In view of the different signal paths from each of the satellites, atmospheric delay errors should not produce such high correlations.

The peak in the residual curves in Figure 4.1 at approximately 489300 occurs at the point where the actual tracking of satellite 6 ceases. A large number of cycle slips and missing observations occur in the final 250

seconds of satellite 6 phase observations. This data was therefore deleted from the observation files for this study. In addition, satellite 11 crosses from the west to east side of the baseline ROOF to CATA at about 489100 seconds.

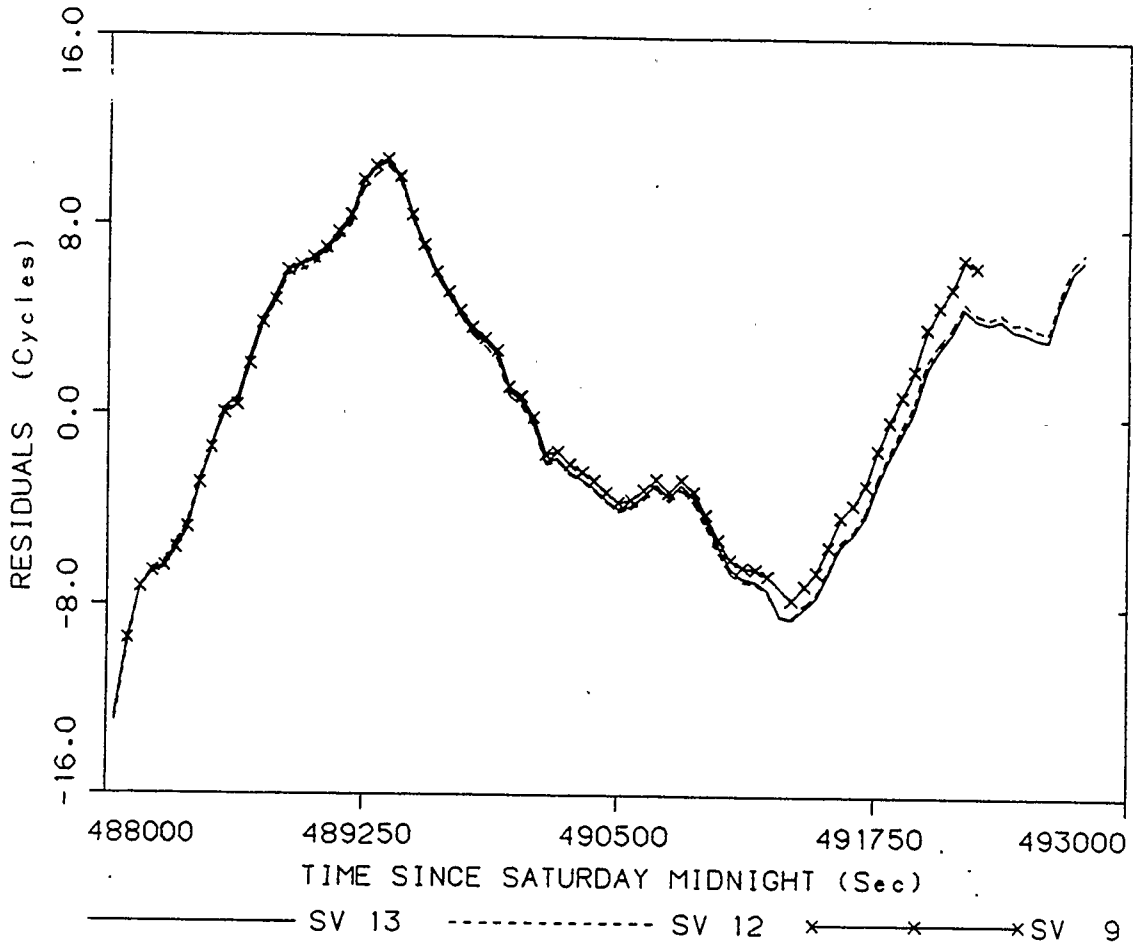


Figure 4.1: Residuals from the Adjustment of Baseline ROOF to CATA

The pattern of the residuals near 489300 seconds suggests that the receivers are changing the clock offset based on differences in the observational data. Variations

of this nature will not be well modelled by a second order polynomial. The local low at approximately 491250 does not occur near changes in satellite tracking or significant losses of lock. The only explanation that can be offered for its occurrence is that satellite 12 reaches the point of closest approach at this time.

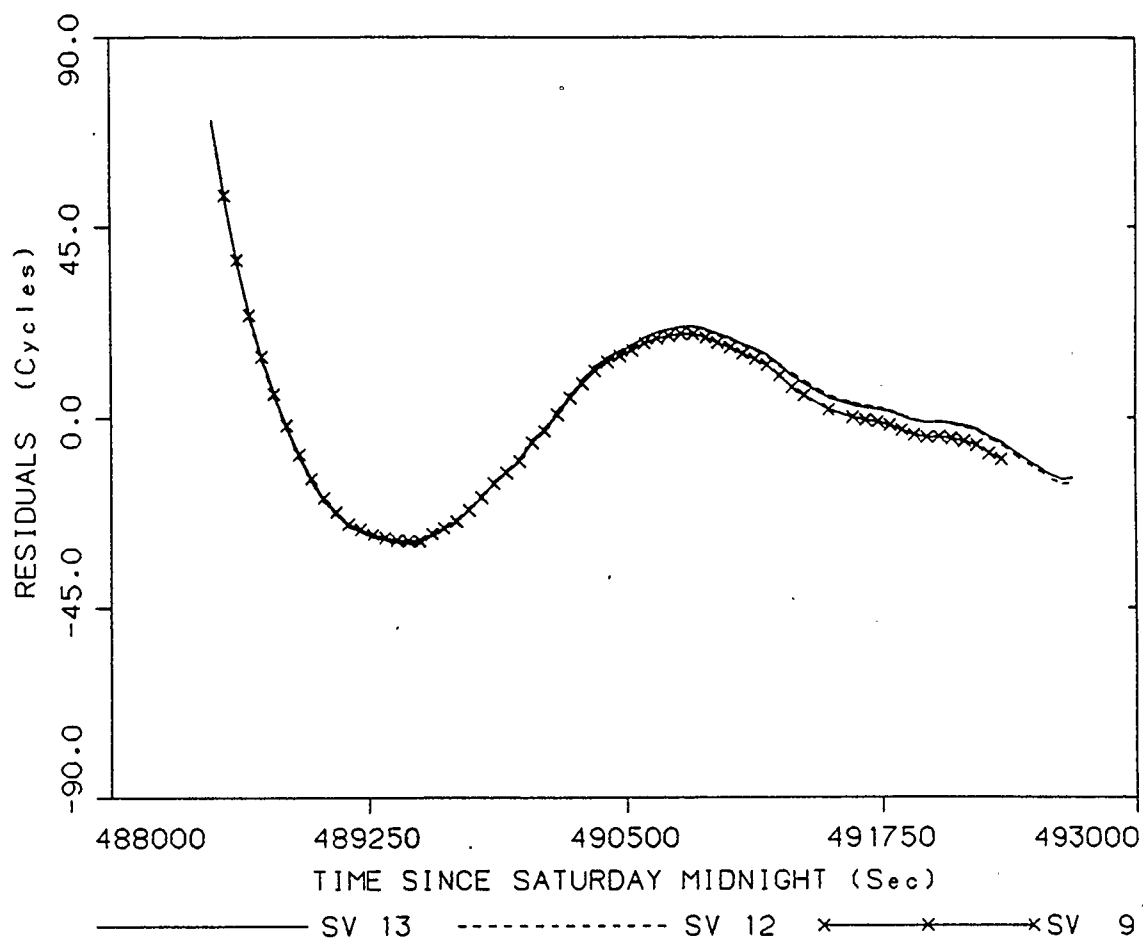


Figure 4.2: Residuals from the Adjustment of Baseline ROOF to METC

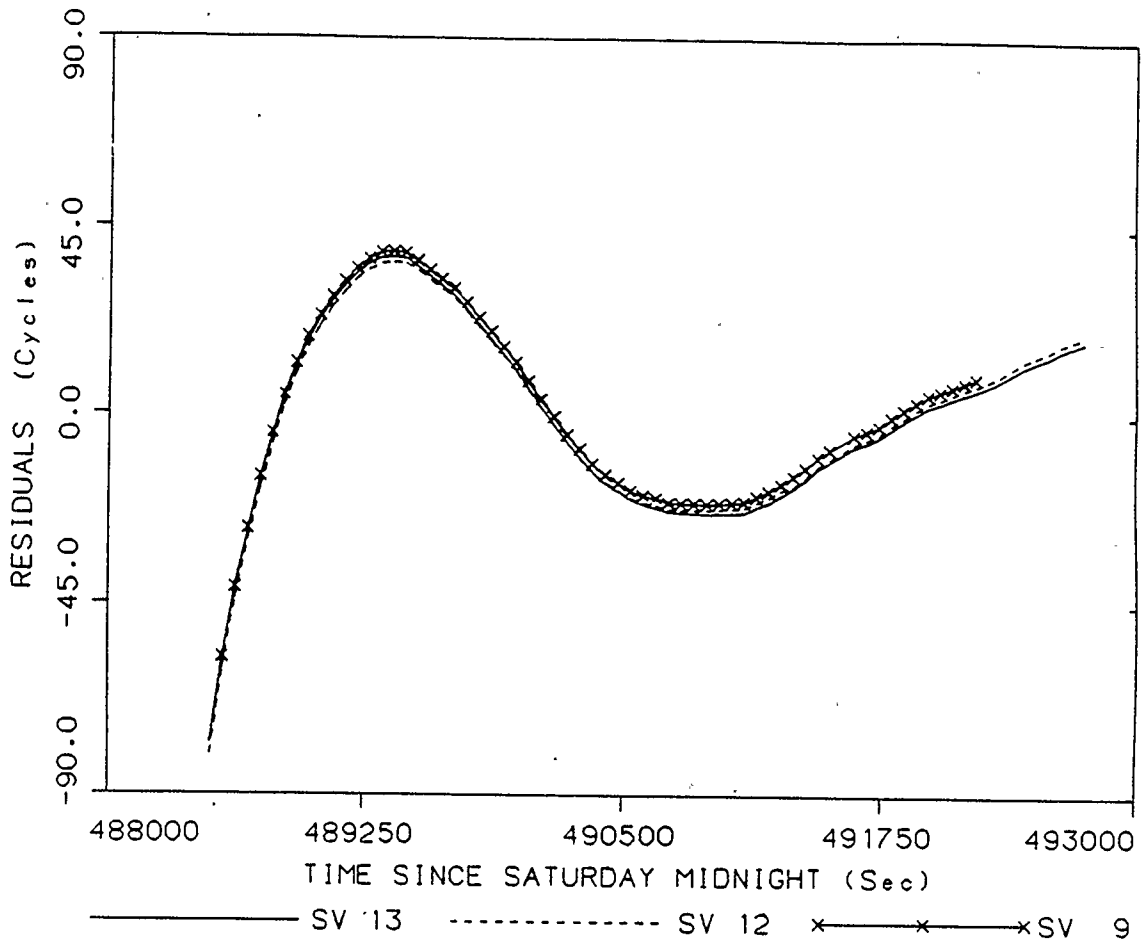


Figure 4.3: Residuals from the Adjustment of Baseline METC to CATA

The excessive magnitude of the residuals on two of the baselines suggests that the receiver at station METC is not performing well. This is also reflected in the results for the station coordinates. Results of the double difference adjustments from the TRIMBLE/TRIMVEC test (McArthur, 1987) show no major problems on these baselines. As a first approximation, the double difference residuals will be the

difference between each of the residual curves. Double difference adjustments will be investigated further in Chapter 6.

The degree of statistical interdependence of the unknown parameters can be estimated by computing the correlation coefficient from the covariance matrix of the adjustment. The correlation coefficient,  $\rho_{ij}$  is given by

$$\rho_{ij} = \frac{\sigma_{ij}}{\sigma_i \sigma_j} , \quad (4.2)$$

where  $\sigma_{ij}$  is the covariance between the unknowns,  $i$  and  $j$ . The terms  $\sigma_i$  and  $\sigma_j$  are the standard deviations of the parameters (Vanicek and Krakiwsky, 1986).

The upper diagonal of the correlation coefficient matrix for run 4.1 (baseline ROOF to CATA) is given in Table 4.3. Linear dependence is exhibited between clock polynomial coefficients of the same order. The linear dependence arises from the fact that the receiver clock offset is split into two polynomials with coefficients of equal magnitude but opposite sign. Very high correlation is also present between all ambiguity terms. The low correlation between the receiver clock coefficients, ambiguities and the station coordinates reflects the initial weighting of the



polynomials not the true correlation between these terms. Note the high correlation between the zeroth-order clock coefficients and the ambiguities. Since these terms are very similar, the high correlation is expected. The almost perfect correlation between the ambiguities indicates that the adjustment does not separate the terms well.

The modification of the polynomial receiver clock model, as discussed in section 2.2 will reduce the high correlations between the coefficients and reduce the singularity problem. More reasonable a priori weights can then be applied to the receiver clock polynomials. Adjustments with the new receiver clock model are presented in the next chapter.

## CHAPTER 5

### POSITIONING RESULTS WITH MODEL VARIATIONS

Section 2.2 proposed a modification of the receiver clock polynomials to account for time-tag errors. In view of the smoothly changing nature of this model, the systematic trend in the residuals will not be completely removed. A first-order Gauss-Markov model will be added to the new polynomial clock model to remove the systematic trend.

#### 5.1 Revised Polynomial Receiver Clock Model

The correlation coefficient matrix presented in Table 4.3 shows fairly high correlations between the ambiguity terms and the zeroth-order clock polynomial coefficients. The effects of time-tag errors are also not accounted for in the original receiver clock model. The receiver clock model presented in section 2.2 will reduce the effects of these time-tag errors. Correlations between the corresponding polynomial coefficients will also be reduced.

Results of the adjustments with the new clock model implemented are presented in Table 5.1. Run 5.1 corresponds to baseline ROOF to CATA, Run 5.2 is ROOF to METC and Run 5.3 is METC to CATA. The initial weighting of the unknowns was kept the same as runs 4.1 to 4.3 to allow a comparison between the correlation coefficient matrices. In each of the adjustments, the GSC published coordinates were entered as the initial estimate of the station coordinates.

The results of the ROOF to CATA adjustment are essentially the same as run 4.1. ROOF to METC shows a significant improvement while a significant decrease in the accuracy of baseline METC to CATA has been obtained. The common clock error determined in the adjustments is approximately  $10^{-12}$  seconds with a drift of  $10^{-12}$  seconds per second. The clock difference has a constant term of approximately  $10^{-11}$  seconds with a drift of  $10^{-10}$  seconds per second. These clock offsets are smaller than expected. Normally they are in the microsecond range with milliseconds being possible. Part of the receiver clock offset is likely being absorbed in the estimate of the ambiguities and the station coordinates. The difference between the results of these adjustments and those presented in chapter 4 are also much larger than can be predicted from time-tag corrections of this magnitude.

Table 5.1: Baseline Errors from Adjustments With  
An Updated Polynomial Receiver Clock Model

Run Number	X	Errors in m and (ppm)			Length
		Y	Z	Pos.	
5.1 R-C	-0.379 (8.4)	-0.114 (1.1)	0.044 (0.5)	0.398 (2.8)	0.173 (1.2)
5.2 R-M	0.711 (32.6)	-2.356 (323.)	-0.569 (46.1)	2.526 (96.8)	1.522 (58.3)
5.3 M-C	2.905 (43.3)	-3.482 (36.3)	0.707 (9.1)	4.589 (32.7)	-0.602 (4.3)
Close	3.995 (29.8)	-5.724 (27.7)	0.092 (0.5)	6.981 (22.5)	0.747 (2.4)
5.4	-0.019 (0.4)	-0.105 (1.0)	0.071 (0.8)	0.128 (0.9)	0.037 (0.3)
5.5	-0.379 (8.4)	-0.114 (1.1)	0.044 (0.5)	0.398 (2.8)	0.173 (1.2)
5.6	0.021 (0.5)	-0.479 (4.6)	0.035 (0.4)	0.481 (3.3)	0.315 (2.2)

The residuals from runs 5.1 to 5.3 are nearly identical to those of runs 4.1 to 4.3. The difference in the results is due to changes in the estimated ambiguities, clock polynomials and accounting for the time tag errors.

The misclosure obtained on the triangle ROOF-METC-CATA-ROOF is shown in Table 5.1. The misclosure on the baseline length is good but the components and overall position error are unacceptable.

The correlation coefficient matrix for run 5.1 is presented in Table 5.2. The coefficients of the common clock error and clock difference are represented by  $x_j$  and  $d_j$ , respectively. The subscript indicates the order of the coefficient. The correlation between the two polynomials has been significantly reduced. Correlation between the zeroth-order coefficient of the clock difference polynomial and the ambiguities is now much higher. The zeroth-order common clock error does not show the same problem.

The very high correlation between the zeroth-order clock difference polynomial and the ambiguities can be reduced by fixing the ambiguities or treating them as weighted parameters. Fixing the zeroth-order term will completely remove the problem. Treating the ambiguities as weighted parameters has the benefit of providing a good starting value for the random process while allowing for estimation errors. Normally, the ambiguities can be estimated by performing an adjustment with both stations held fixed. The coordinates for one of the stations will be determined from the double difference adjustment in the preprocessor, hence some error is to be expected in the estimated values of the ambiguities. The almost perfect correlation between the ambiguities also indicates that they cannot be separated by the adjustment.



Adjustments of each of the baselines, with both stations held fixed were run to determine good estimates of the ambiguities and the clock polynomial coefficients. The GSC published values of the station coordinates were entered for both stations. Therefore, the estimates of the unknowns will be of good accuracy.

To determine the possible extent by which the station coordinate errors can be improved by adding ambiguity a priori information, the baseline ROOF to CATA was readjusted with the new ambiguities held fixed. The new estimates of the receiver clock polynomial coefficients were also entered with reduced initial variances. Results of this adjustment are listed in Table 5.1, denoted run 5.4. These results are very good but much of the input information was from well known station positions.

Fixing the constant term of the clock difference polynomial will correct the problem of the high correlation with the ambiguities. The  $d_0$  term should be fixed at the value determined in the adjustment with both stations held fixed. The time-tag errors resulting from this clock offset can therefore be accounted for.

Results of an adjustment of the baseline ROOF to CATA, with the  $d_0$  term fixed are shown in Table 5.1, denoted run

5.5. The station coordinate errors are identical to those of run 5.1. Fixing the  $d_0$  term has no adverse affect on the adjustment if an initial estimate of the term is supplied and the ambiguities are solved for as free parameters.

The correlation coefficient matrix from run 5.5 is presented in Table 5.3. The correlations between the ambiguities have been significantly reduced. Correlations between the ambiguities and the station coordinates are now in the range expected. Adding weights to the a priori estimates of the ambiguities will reduce these correlations.

The discussion in chapter 4 suggested that poor satellite geometry in the later part of the data set could be part of the cause of the poor results. To test this theory, the baseline ROOF to CATA was readjusted with only the first 1000 seconds of data. This section of data has five satellite coverage and a GDOP of 4.5. Results of this adjustment are shown in Table 5.1, denoted run 5.6. The station coordinate errors are slightly larger than those of run 5.1. Therefore, poor satellite geometry cannot be the major contributor to the poor results.

The residuals from run 5.6 are plotted in Figure 5.1. Comparing Figures 5.1 and 4.1 shows that the residuals from the shorter data set are the higher frequency fluctuations



in the residual curve of the longer data set. The satellite geometry is essentially constant in the shorter data set; therefore, the receiver's estimate of the clock offset is affected only by oscillator drift and noise. In the longer data set, the satellite geometry changes; therefore, the receiver's estimate of the clock offset is changing. This gives rise to the systematic trend in the residuals.

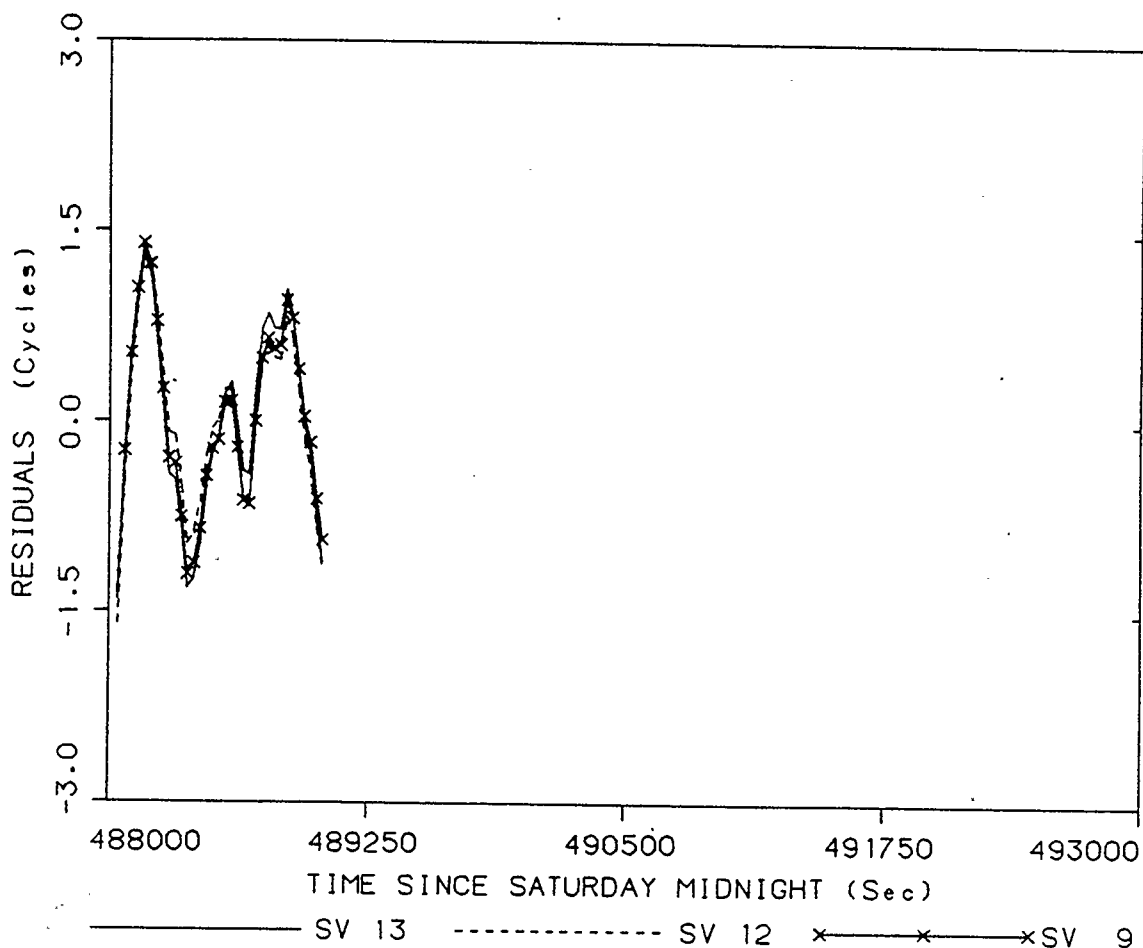


Figure 5.1: Residuals from the Adjustment of Baseline ROOF to CATA, Run 5.6

In summary, the analysis up to this point has shown that:

- 1) the adjustment can be improved by adding a priori information about the magnitude of the ambiguities,
- 2) the very high correlation between the ambiguities and the constant term of the clock difference polynomial can be removed by fixing the  $d_0$  coefficient at the a priori determined value,
- 3) receiver clock errors are not well modelled by the second-order polynomials,
- 4) and the section of poor satellite geometry is not a major contributor to the poor positioning results.

Adjustments with weighted ambiguities are investigated in section 5.2. The large systematic trend in the residuals will be reduced by incorporating a first-order Gauss-Markov process. Results of adjustments with a Gauss-Markov process implemented are presented in section 5.3.

## 5.2 Adjustments with Weighted Ambiguities

The analysis in the previous section showed that the results of the adjustments can be improved if an initial estimate of the ambiguities is supplied. In a production survey, the ambiguities can be determined from double or triple difference adjustments or from holding both stations

fixed in a single difference adjustment. Treating the ambiguities as weighted parameters will account for errors in the estimated values.

The first attempt at adjusting the data from the baseline ROOF to CATA with weighted ambiguities was unsuccessful. No convergence was achieved in 35 iterations with the station coordinate convergence tolerance set at 0.002 m. The adjustment was approaching convergence but very slowly. The clock polynomial coefficients were also converging very slowly.

In this adjustment, an initial variance of two cycles squared was applied to each ambiguity. Covariance between the ambiguities was neglected. The two cycles squared variance assumes that the station positions were accurate to better than 0.5 m in the adjustment to determine the ambiguities. The initial estimates of the clock polynomial coefficients were obtained from the adjustment with both stations held fixed. The  $d_0$  clock term was also held fixed.

Raising the station coordinate convergence tolerance to 0.004 m and repeating the adjustment produces the results shown in Table 5.4, denoted run 5.7. Convergence was achieved in 17 iterations. The position errors have improved over those of run 5.1 but a convergence problem has now

appeared. The adjustment is attempting to reach the solution of run 5.1 but weighting of the ambiguities is only allowing small movements in each iteration step. The station coordinates are highly correlated with the ambiguities, therefore the station position cannot move substantially in each iteration, since the ambiguities are constrained.

Table 5.4: Baseline Errors from Adjustments  
With Weighted Ambiguities

Run Number	X	Errors in m and (ppm)			Length
		Y	Z	Pos.	
5.7	-0.260 (5.7)	-0.124 (1.2)	0.036 (0.4)	0.290 (2.0)	0.193 (1.3)
5.8	-0.273 (6.0)	-0.235 (2.3)	0.026 (0.3)	0.361 (2.5)	0.238 (1.6)

Weighting the ambiguities reduces the correlation with the zeroth-order clock difference polynomial coefficient. Reintroducing this term into the adjustment to absorb some of the error in the ambiguities slightly alleviates the convergence problem. Unfortunately, the results of this adjustment are slightly inferior to those of run 5.7 (see Table 5.4, Run 5.8).

The initial convergence tolerance of one or two millimetres may be too low given the noise inherent in the observations and model uncertainties. Implementing the

Gauss-Markov receiver clock model may reduce this problem in addition to removing the systematic trend seen in the residuals. The next section discusses Gauss-Markov models and presents results of adjustments with the random process incorporated.

### 5.3 Gauss-Markov Receiver Clock Model

A Gauss-Markov process is a special case of a random process which can be produced by applying white noise to a linear feedback system. It fits a large number of physical processes with reasonable accuracy while the mathematical description is relatively simple (Brown, 1983).

Markov processes are affected by the preceding events but the effect of these events on the current state diminishes in time until they are forgotten (Davis, 1986). A process is first-order Markov if the probability distribution of the process  $X(t_k)$  is dependent only on the last data value. A first-order Markov process is also referred to as a first-order autoregressive (AR) process (Jenkins and Watts, 1968). The process is called Gauss-Markov if the probability distribution functions of the white noise  $W$  and the series  $X$  are also Gaussian (Gelb, 1974). Specifying the autocorrelation function completely describes the statistics of a stationary Gauss-

Markov process (Brown, 1983). The next section will present a brief outline of AR processes.

### 5.3.1 Discussion of the Autocorrelation Function And Gauss-Markov Processes

The autocovariance function (acvf) of a stationary process  $X_t$  with zero mean is defined as

$$C_x(u) = \text{Cov}[X_t, X_{t+u}], \quad (5.1)$$

where  $\text{Cov}[]$  indicates the covariance between the values of the series,  $u$  points apart. The displacement  $u$  is called the lag. The acvf depends on the scale of the series  $X$  therefore the autocorrelation function (acf), defined as

$$R_x(u) = \frac{C_x(u)}{C_x(0)}, \quad (5.2)$$

allows comparison of two series with different scales of measurement. Both the acf and acvf are functions of the lag only (Jenkins and Watts, 1968). The acvf and acf will be denoted  $C_u$  and  $R_u$  respectively.

An unbiased estimate of the acvf for a discrete time series with zero mean may be computed from

$$C_u = \frac{1}{N-u} \sum_{t=1}^{N-u} X_t X_{t-u}, \quad u = 0, 1, \dots, N-1, \quad (5.3)$$

or alternately, a biased estimate of the acvf may be computed from

$$C_u = \frac{1}{N} \sum_{t=1}^{N-u} X_t X_{t-u}, \quad u = 0, 1, \dots, N-1, \quad (5.4)$$

where  $N$  is the number of data points in the series. The benefit of using equation (5.4) over (5.3) is that the error in the estimate is reduced for larger lags. As  $u$  approaches  $N$ , the variance of the biased estimator approaches zero while the variance of the unbiased estimator approaches infinity (Jenkins and Watts, 1968).

The  $p$ -th order AR model of a discrete process  $X_t$  may be written (Box and Jenkins, 1970)

$$X_t = P_1 X_{t-1} + P_2 X_{t-2} + \dots + P_p X_{t-p} + W_t, \quad (5.5)$$

where  $W_t$  is the input white noise and the AR parameters,  $P_i$ , represent a finite set of weights. Multiplying equation (5.5) by  $X_{t-u}$  and taking expected values yields

$$R_u = P_1 R_{u-1} + P_2 R_{u-2} + \dots + P_p R_{u-p}, \quad u > 0. \quad (5.6)$$

The acf obeys the same difference equation as the series.

The values of the AR parameters are determined by forming a set of linear equations from (5.6) that are known as the Yule-Walker Equations (Box and Jenkins, 1970)

$$\mathbf{P} = (\mathbf{A}^T \mathbf{A})^{-1} \mathbf{A}^T \mathbf{R}, \quad (5.7)$$

where

$$\mathbf{P} = \begin{bmatrix} P_1 \\ P_2 \\ \vdots \\ P_p \end{bmatrix} \quad \mathbf{R} = \begin{bmatrix} R_1 \\ R_2 \\ \vdots \\ R_N \end{bmatrix} \quad (5.8)$$

$$\mathbf{A} = \begin{bmatrix} 1 & R_1 & R_2 & \dots & R_{p-1} \\ R_1 & 1 & R_1 & \dots & R_{p-2} \\ R_2 & R_1 & 1 & \dots & R_{p-3} \\ \vdots & \vdots & \vdots & \ddots & \vdots \\ \vdots & \vdots & \vdots & \ddots & \vdots \\ R_{N-2} & R_{N-3} & R_{N-4} & \dots & R_{N-p-1} \\ R_{N-1} & R_{N-2} & R_{N-3} & \dots & R_{N-p} \end{bmatrix}$$

In the foregoing, the Yule-Walker equations have been extended to allow for redundant information. Equations (5.8) utilize the properties of the autocorrelation and autocovariance functions;  $R(0)=1$  and  $R(-u) = R(u)$ .

From equation (5.5), the first order Gauss-Markov process is given by

$$X_t = P_1 X_{t-1} + W_t, \quad (5.9)$$

where  $-1 < P_1 < 1$  if the process is stationary. The acf can be expressed as

$$R_u = P_1 R_{u-1} . \quad (5.10)$$

With  $R_0 = 1$ , equation (5.10) has the solution  $R_u = P_1^u$ . This autocorrelation function decays exponentially to zero if  $P_1$  is positive (Box and Jenkins, 1970). The acf of a first order Gauss-Markov process can therefore be expressed in the form given by Gelb, (1974)

$$R_u = \exp(-\beta u) \quad (5.11)$$

where  $\exp(-\beta u)$  is the exponential function with an exponent of  $(-\beta u)$ ,  $1/\beta$  is the correlation time (1/e point). The value of the correlation time can be determined by performing an adjustment of equation (5.11) with  $R_u$  computed from either equation (5.3) or (5.4). The discrete version of the prediction equation is now written

$$X_k = X_{k-1} \exp[-\beta(t_k - t_{k-1})] + W_k . \quad (5.12)$$

Equations (5.11) and (5.12) are implemented in the adjustment software package to model the receiver clock offset. The receiver clock polynomial now forms the deterministic part of the clock model while the Gauss-Markov process forms the stochastic part.

The residual computed from the first observation to each satellite is used as the starting value of the series. The first observations to each satellite are not summed into the normal equations. Equation (5.12) is used with the initial value to estimate the bias for the next observation. The estimated bias is removed from the observation during the computation of the misclosure. The current value of the series is then updated based on the actual measurement.

### 5.3.2 Initial Baseline Results with a Gauss-Markov Clock Model Implemented

The acf obtained with the unbiased estimator from the satellite PRN 13 residuals of the fixed stations adjustment of baseline ROOF to CATA is shown in Figure 5.2 along with the 95% confidence limits (dashed lines). The confidence limits are computed from the large N approximation,  $\text{Var}[R_u] = 1/(N - u)$ , given in Yule and Kendall (1950). Only the autocorrelations with a magnitude greater than zero were used to estimate the correlation time. Performing the adjustment using equation (5.11) as the mathematical model yields a correlation time of 553.8 seconds. The correlation time for baseline ROOF to METC was 372.5 seconds and 357.8 seconds for baseline METC to CATA.

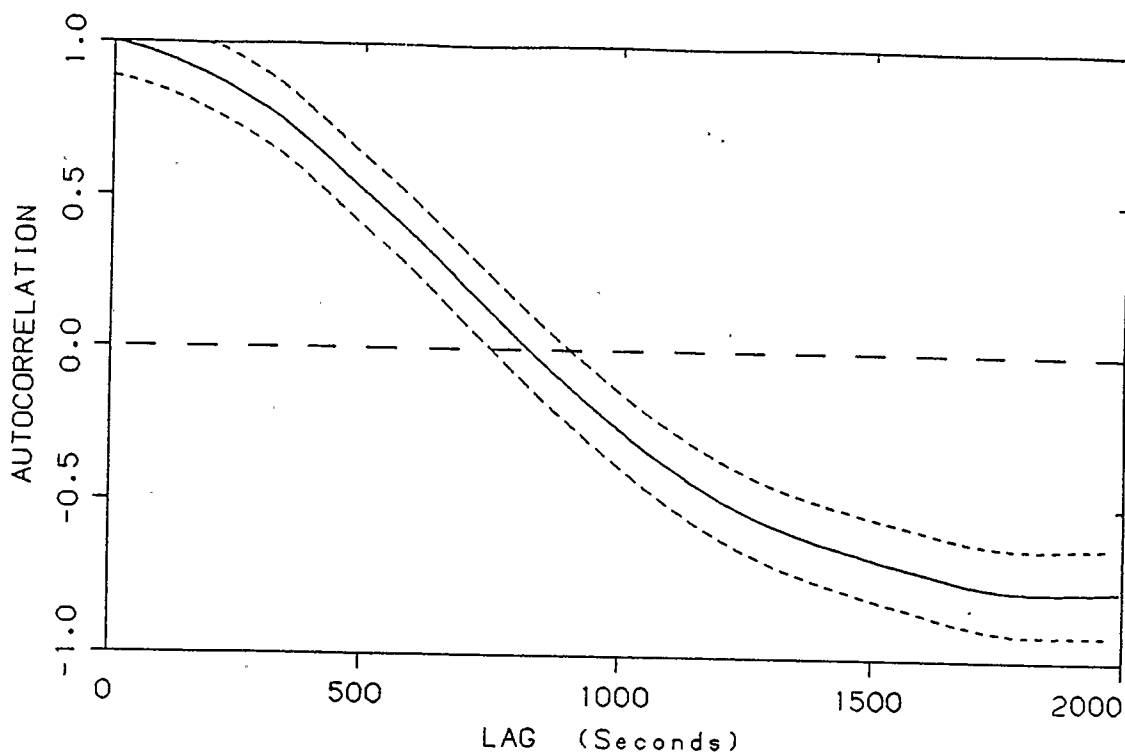


Figure 5.2: Autocorrelation Function of Satellite 13 Residuals, ROOF to CATA Fixed Stations Adjustment

The first attempt to readjust the data from the baseline ROOF to CATA with a first order Gauss-Markov model implemented was unsuccessful. In this adjustment, the ambiguities were solved for as free parameters and the station coordinates were given a variance of  $25 \text{ m}^2$ . In view of the results in section 5.2, the zeroth-order term of the clock difference polynomial was held fixed. The estimate of

the  $d_0$  term was obtained from the fixed stations adjustment. The initial values of the other polynomial coefficients were also obtained from the fixed station adjustment. No convergence was obtained at the 0.020 m level for the station coordinates. It also appears that the estimates of the receiver clock coefficients are converging much slower than in previous runs. The coefficients have become insensitive to changes as a result of incorporating the Gauss-Markov process. This is a direct result of estimating the Gauss-Markov predictions in each iteration.

Treating the ambiguities as weighted parameters with a variance of two cycles squared resulted in similar problems. Entering an estimate of the ambiguities provides better starting values for the predictor but the convergence problems have been compounded.

Once again, the clock parameters also exhibited convergence problems. Convergence of the adjustment was obtained by modifying the input information and convergence tolerance. The weights applied to the clock polynomial coefficients were increased and the convergence tolerance was set at 0.020 m. Convergence was obtained in 21 iterations. The results for this adjustment (Run 5.9) are presented in Table 5.5. The derived station position of Run

5.9 is of lower accuracy than previous adjustments, although the convergence is better.

The interaction between the Gauss-Markov process and the two polynomial clock models is creating an unstable adjustment. To remove the interaction, the adjustment was rerun with all of the clock polynomial coefficients held fixed. Errors in the station position from this adjustment are shown in Table 5.5, designated Run 5.10. The convergence problem has been further aggravated. The adjustment required eleven iterations to converge at the 0.040 m level. No convergence was obtained at the 0.020 m level in 35 iterations. Comparing the results of runs 5.9 and 5.10 also shows a significant difference.

A plot of the residuals from three of the satellites in run 5.9 is presented in Figure 5.3. The correlation coefficient is shown in Table 5.6. The first order Gauss-Markov process has reduced the maximum size of the residuals by almost an order of magnitude although a long-term systematic trend still exists. Superimposed on this trend is high frequency noise. Reducing the correlation time of the Gauss-Markov process will reduce the level of the high frequency noise but increase the amplitude of the systematic trend. In addition, interaction between the random process

and the receiver clock polynomial will be reduced. Thus, part of the convergence problem can be alleviated.

Table 5.5: Baseline Errors from Adjustments with a Gauss-Markov Process Implemented

Run Number	Errors in m and (ppm)				
	X	Y	Z	Pos.	Length
5.9	0.253 (5.6)	0.514 (5.0)	0.097 (1.1)	0.581 (4.0)	-0.508 (3.5)
5.10	-0.026 (0.6)	-0.169 (1.6)	0.552 (5.8)	0.549 (3.8)	-0.196 (1.4)
5.11	-0.035 (0.8)	0.046 (0.4)	0.226 (2.5)	0.233 (1.6)	-0.163 (1.1)
5.12	0.039 (0.9)	0.169 (1.6)	-0.112 (1.2)	0.206 (1.4)	-0.063 (0.4)
5.13 R-C	0.010 (0.2)	-0.052 (0.5)	0.087 (1.0)	0.102 (0.7)	-0.020 (0.1)
5.14 R-M	0.174 (8.0)	-0.055 (7.5)	0.185 (15.0)	0.260 (10.0)	0.073 (2.8)
5.15 M-C	-0.134 (2.0)	-0.163 (1.7)	-0.053 (0.7)	0.218 (1.5)	0.205 (1.5)
Close	0.030 (0.2)	-0.166 (0.8)	0.045 (0.3)	0.175 (0.6)	0.298 (1.0)
Tr/Trim R - C	-0.189 (4.2)	-0.053 (0.5)	-0.306 (3.4)	0.364 (2.5)	0.093 (0.6)
Tr/Trim R - M	-0.010 (0.5)	0.134 (18.4)	0.083 (6.7)	0.158 (6.1)	-0.085 (3.3)
Tr/Trim M - C	-0.178 (2.7)	-0.178 (1.9)	0.222 (2.9)	0.336 (2.4)	0.084 (0.6)



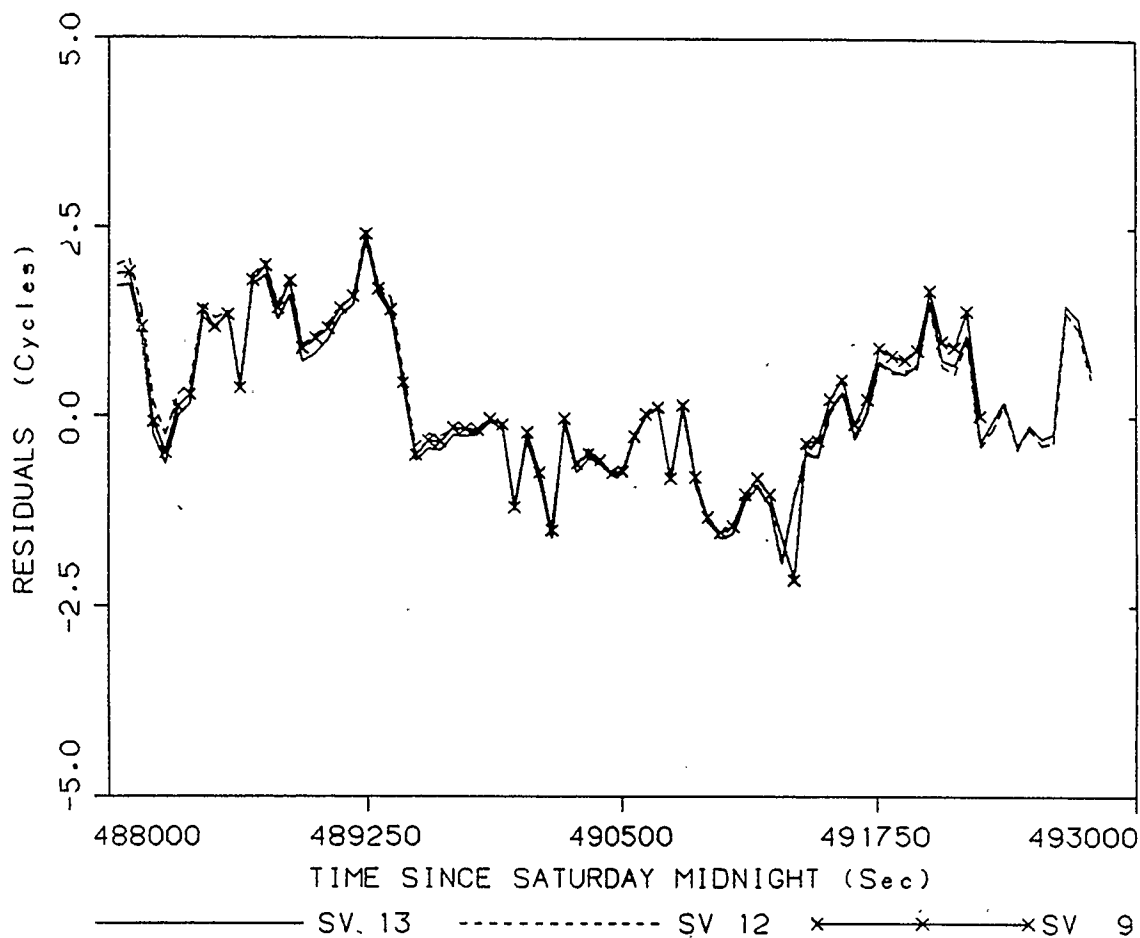


Figure 5.3: Residuals from the Adjustment of Baseline ROOF to CATA with a Gauss-Markov Clock Model

Arbitrarily choosing a correlation time of twice the data rate, i.e. 120 seconds, and readjusting the data from baseline ROOF to CATA yields the results shown in Table 5.5, run 5.11. The ambiguities were solved for as weighted parameters with an a priori variance of two cycles squared. Coefficients for both the receiver clock polynomials were solved for, except the zeroth order clock difference term

which was held fixed. Convergence at the 0.010 m level was achieved in 21 iterations. The shorter correlation time has removed much of the convergence problem but not completely corrected it. No convergence was obtained at the 0.002 m level in 35 iterations.

Station position errors from run 5.11 are now very good. Residuals from this adjustment are shown in Figure 5.4. The shorter correlation time has removed much of the high frequency noise but the amplitude of the long-term trend has increased. Additional terms can be added in the polynomial clock model to remove this trend but this is likely to further aggravate the convergence problems. Typically, the receiver clocks exhibit behaviour that can be described by an offset from true GPS time and a linear drift. A small quadratic trend may also be superimposed on the linear trend (Remondi, 1984). Therefore, the higher order trends are difficult to justify physically.

Estimating the clock offsets as a white noise process should remove the majority of clock trend but significantly increase the number of unknowns. Alternatively, the receiver clock offsets can be determined from a single point pseudorange solution. The estimated clock offsets can then be removed for the carrier beat phase observables prior to forming the single differences. This technique will add a

high degree of noise to the observations but it may successfully remove the large systematic trend.

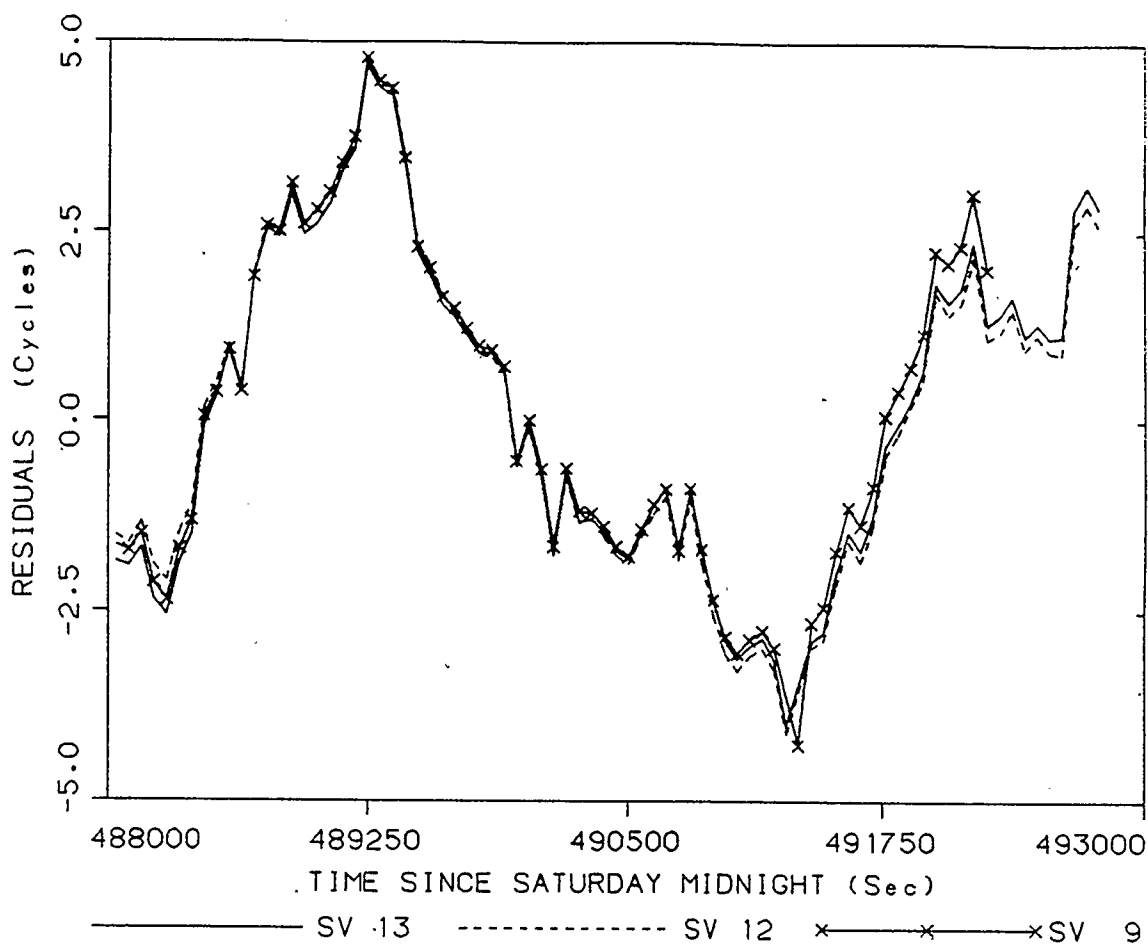


Figure 5.4: Residuals from the Run 5.11 Adjustment

Treating the ambiguities as weighted parameters has resulted in convergence problems throughout the preceding analysis. Treating the ambiguities as fixed parameters will reduce the convergence problems. To test this theory, run 5.10 was repeated with the ambiguities held fixed. The clock

polynomial coefficients, excluding  $d_0$ , were also solved for. Convergence was obtained at the 0.002 m level in eight iterations. The results, shown in Table 5.5 (Run 5.12) are very good and the convergence problem has been significantly reduced.

Since both the ambiguities and the  $d_0$  term are fixed, any unmodelled constant clock effects are likely absorbed in the estimates of the station coordinates. In an attempt to further improve the results, the adjustment was repeated while solving for the entire clock polynomial. The station position errors show a further increase in accuracy, see Run 5.13, Table 5.5.

The data from the other baselines was also readjusted with fixed ambiguities and solving for the full polynomial clock model. The results are presented in Table 5.5. Run 5.14 corresponds to baseline ROOF to METC, while baseline METC to CATA corresponds to run 5.15. The coordinate errors on each of these baselines show a significant improvement over that of Runs 5.1 to 5.3. The position errors are now acceptable for each of the baselines. The closure of the triangle, shown in Table 5.5 is also within an acceptable range. Table 5.5 also shows the results obtained in the TRIMBLE/TRIMVEC test (McArthur, 1987) for comparison.

It should be noted that the ambiguities used in Runs 5.13 to 5.15 were determined from an adjustment with both stations held fixed at their published values. They were also not rounded to the nearest integer value. In a production survey, the initial estimate of the ambiguities cannot be determined to this accuracy. As an alternative, the estimated ambiguities can be rounded to integer values while allowing the clock polynomials and random process to absorb the constant part of the receiver clock offset. An integer ambiguity search can then be performed to determine the correct values.

In summary, good results can be obtained with the program package but an accurate knowledge of the ambiguities is required. A reasonable estimate of the clock polynomial coefficients is also required. Treating the ambiguities as free parameters results in large position errors while entering the ambiguities as weighted parameters produces convergence problems. The convergence problems may be due to model uncertainties and measurement noise.

Only short correlation times can be chosen for the Gauss-Markov receiver clock model. Longer correlation times produce convergence problems although the magnitude of the systematic trend in the residuals is greatly reduced.

Part of the model uncertainties that produce the convergence problems may be due to the simultaneous transmit time formulation. As noted in Chapter 2, the clock offset errors contributed by the dissimilar received times should be negligible. This bias error should be removed by the clock polynomial and random process. In the following chapter, two double difference adjustments are used to test the effects of the simultaneous received time model. One adjustment is formulated on the basis of simultaneous transmit times while the other uses simultaneous received times.

## CHAPTER 6

### DOUBLE DIFFERENCE ADJUSTMENTS

Double differenced observations remove most of the effect of the receiver clock errors. In theory, the entire clock error is removed only if all four carrier beat phase observations have identical received times. Forming double difference observations from the single differences that are used in ASTRO will not completely remove the clock errors since the four signals are no longer received at identical epochs. Two of the observations will be nearly simultaneous while the remaining two will have different arrival times which are a function of the satellite geometry and baseline orientation. The clock error that remains will contain the effects of the differenced clock bias during the interval between the arrival times.

Two different double difference adjustment programs have been written to determine the effect of the remaining errors on determining the station coordinates. In the first version, the double differences are formed from two of ASTRO's single difference observations. In the second version, the double differences are formed from four one-way

phase observations which have nearly simultaneous received times. In both cases, the correlations between the observations have been properly accounted for.

The following sections present results from adjustments of the data from baseline ROOF to CATA. In all of the forthcoming adjustments, the coordinates of station ROOF have been held fixed. The published coordinates of station CATA were entered as the initial estimate. The convergence criteria for all adjustments was one millimetre for the station coordinates and 0.1 cycles for the ambiguities.

### 6.1 Double Difference Adjustment Results, Version 1

In this version, the double differences are formed from two of the single differences used in ASTRO. Comparing plots of the adjustment residuals with those of the previous chapters will show the extent of the receiver clock errors that are removed by forming the double differences. Comparison of the results with those obtained from the second version and published results of the TRIMBLE/TRIMVEC test (McArthur, 1987) shows the suitability of the model.

Initially, only the station coordinates and ambiguities were solved for. In the first adjustment, all the parameters

were treated as true unknowns. The results are presented in Table 6.1, listed as run 6.1. The correlation coefficient matrix is shown in Table 6.2. Residuals for three of the satellite combinations are plotted in Figure 6.1. This figure shows that the majority of the receiver clock errors exhibited by the SD residuals have been removed (also see Figure 4.1). A small satellite specific trend is now identifiable in the residual curves. This trend is due to the unmodelled receiver clock errors.

The station coordinate errors do not show an improvement over the single difference results (run 5.1) but they are still reasonable. A large percentage of this error can be attributed to the fact that the two single differences have slightly different received times.

Table 6.1: Baseline Errors from Version 1  
Double Difference Adjustments

Run Number	X	Errors in m and (ppm)			Length
		Y	Z	Pos.	
6.1	-0.034 (0.8)	-0.765 (7.4)	0.028 (0.3)	0.776 (5.4)	0.541 (3.7)

The correlation coefficient matrix, Table 6.2, still shows very high correlation between the ambiguities themselves and the station coordinates, similar to the

single difference adjustments. The ability to correctly determine the integer value of the ambiguities and fix them will thus greatly strengthen the adjustment.

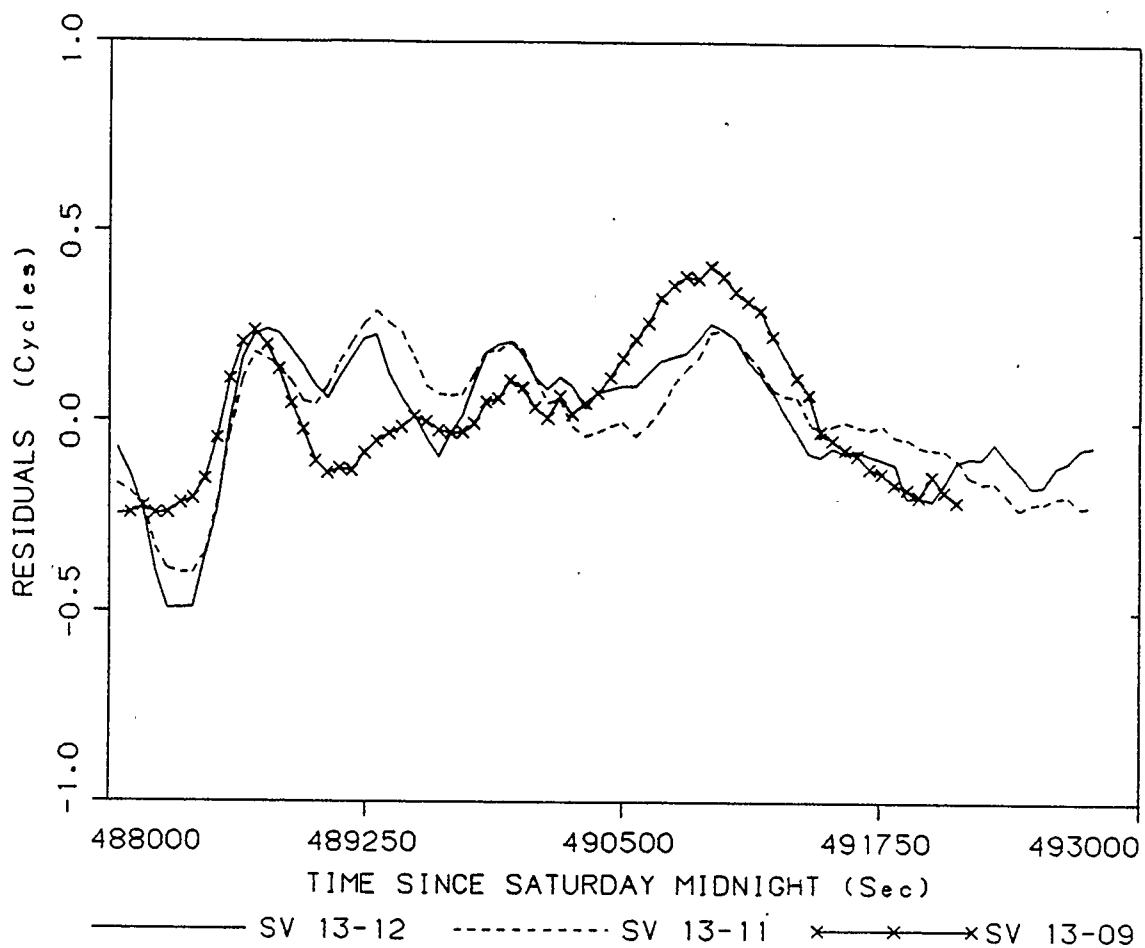


Figure 6.1: Residuals from the Double Difference Adjustment of Baseline ROOF to CATA, Run 6.1

The single difference adjustments became unstable when the estimated ambiguities were treated as weighted parameters. Applying the same two cycle squared variance to

the ambiguities obtained from Run 6.1 and readjusting the data does not produce the same instability. Both Run 6.1 and the weighted ambiguity adjustment converged in two iterations with no change in the convergence tolerance. As expected, the results of the weighted ambiguity adjustment and Run 6.1 show no significant difference.

Table 6.2: Correlation Coefficient Matrix  
for Run 6.1, Baseline ROOF to CATA

	X	Y	Z	N <sub>13-12</sub>	N <sub>13-11</sub>	N <sub>13-9</sub>	N <sub>13-6</sub>
X	1.00	-0.91	-0.39	-0.89	0.99	0.94	0.96
Y		1.00	0.23	0.95	-0.89	-0.95	-0.93
Z			1.00	0.30	-0.35	-0.47	-0.51
N <sub>13-12</sub>				1.00	-0.85	-0.91	-0.91
N <sub>13-11</sub>					1.00	0.92	0.94
N <sub>13-09</sub>						1.00	0.98
N <sub>13-06</sub>							1.00

In an attempt to remove the remaining receiver clock errors, four second order polynomials were added as nuisance parameters. Anticipating that the ambiguities will absorb the constant part of each clock offset, only the linear and quadratic coefficients are solved for. The performance of this adjustment is strongly influenced by the initial weights applied to the parameters. In all cases, convergence

is very slow as a result of the highly correlated polynomial coefficients. The adjustment required 39 iterations to converge and resulted in a significant reduction in the accuracy of the estimated station position. The poor results and convergence problems are a result of high correlations between the polynomial coefficients which indicates an overparameterization of the solution.

## 6.2 Double Difference Adjustment Results, Version 2

In this version, double differences are formed from four one-way phase observations with nearly simultaneous received times. All DD observations with received times differing by more than 0.7 milliseconds were rejected. This is the most commonly implemented formulation for double difference adjustments (Delikaraoglou, 1987). This formulation should remove a greater portion of the receiver clock errors than the previous version.

The mathematical model implemented corresponds to that given in Remondi (1984), similar to the final single difference model. Parameters are included for the station coordinates, ambiguities, unmodelled tropospheric delay scale factor and residual receiver clock error. The receiver clock error is modelled by two second-order polynomials, one for the common clock error and the other for the difference

between the receiver clocks. Time-tag errors are accounted for in the formulation of the clock model.

Initially, only the station coordinates and ambiguities are solved for as true unknowns. The results of this adjustment are listed in Table 6.3, denoted Run 6.2. Fixing the ambiguities at their real values or adding weights of two cycles squared to the ambiguity estimates does not change the coordinate errors or rate of convergence. The results are in approximately the same range as the results of the TRIMBLE/TRIMVEC test (McArthur, 1987) shown in Table 6.4. The results from the version 2 adjustments will likely improve with additional modelling of the error sources, primarily the receiver clock errors.

Table 6.3: Baseline Errors from Version 2  
Double Difference Adjustments

Run Number	Errors in m and (ppm)					Length
	X	Y	Z	Pos.		
6.2	0.038 (0.8)	-0.867 (8.4)	-0.015 (0.2)	0.869 (6.0)	0.618 (4.3)	
TRIMBLE TRIMVEC	-0.189 (4.2)	-0.053 (0.5)	-0.306 (3.4)	0.364 (2.5)	0.093 (0.6)	
6.3	-0.356 (7.9)	-0.170 (1.6)	-0.481 (5.3)	0.622 (4.3)	0.533 (3.7)	

The residuals from three of the satellite combinations of Run 6.6 are presented in Figure 6.2. Note the large number of satellite 13-12 observations that were deleted due to differences in the received times exceeding 0.7 milliseconds. Deleting these observations significantly increases the GDOP in the earlier section of the data set. The less favourable satellite geometry is likely the cause

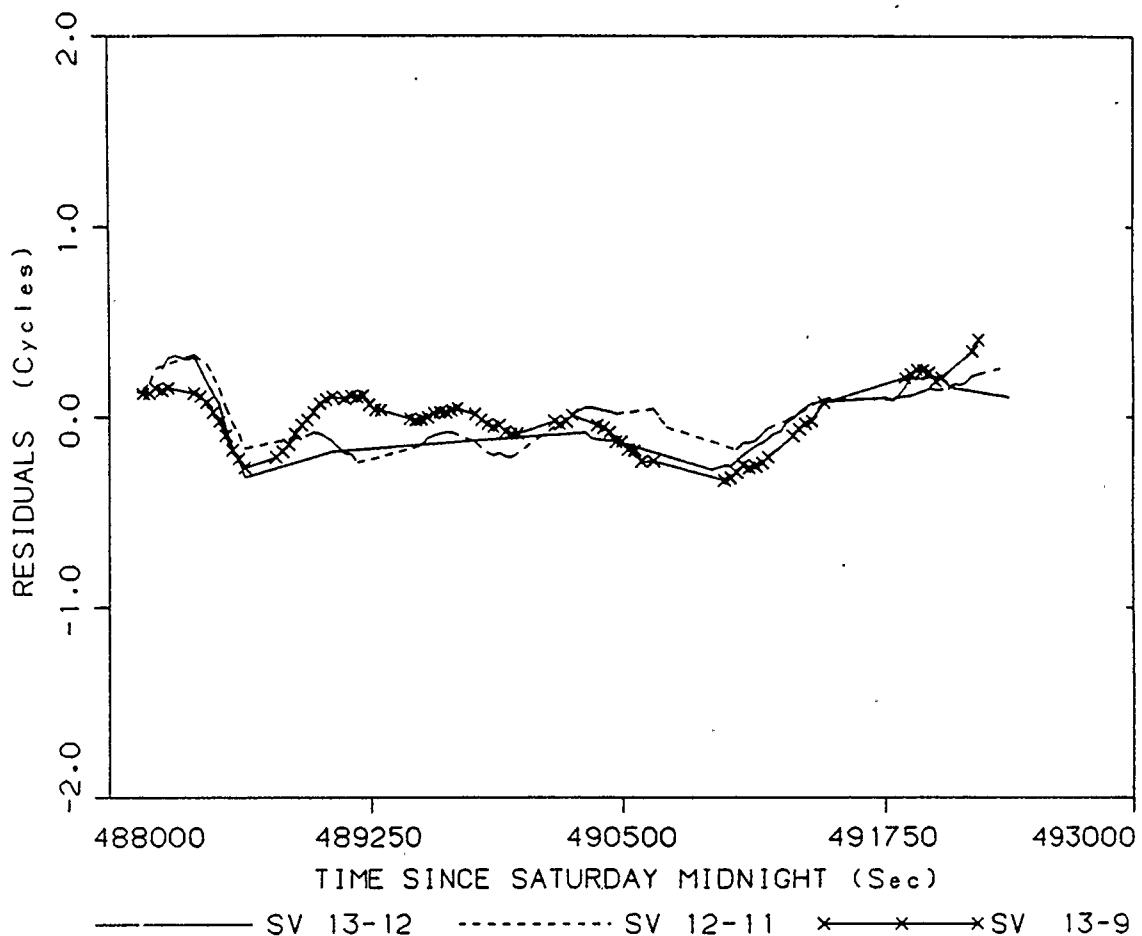


Figure 6.2: Residuals from Double Difference Adjustment of Baseline ROOF to CATA, Run 6.2

of the slight increase in the position errors. Comparing the residuals in Figure 6.1 and 6.2 shows a decrease in the magnitude from the version 2 adjustment. The simultaneous received time formulation is removing more of the clock errors.

To further explore the effects of the receiver clock errors, the version 2 adjustment was repeated with both clock polynomials and the tropospheric delay scale factor included as nuisance parameters. Once again, this adjustment is affected by the weights of the initial estimates although not to the same degree as the version 1 adjustment.

The results are listed in Table 6.4, denoted Run 6.3. A comparison of the residuals from Runs 6.2 and 6.3 for satellite combination 13-11 is shown in Figure 6.3. The residuals from Run 6.2 are shown with the solid line while the dashed line corresponds to Run 6.3.

The magnitude of the residuals does not change significantly between the two adjustments but the station coordinate errors change dramatically. Obviously, the unmodelled receiver clock errors are being absorbed in the estimate of the station coordinates in Run 6.2. Since double difference adjustments are relatively insensitive to

receiver clock errors, the effect must be magnified in a single difference adjustment.

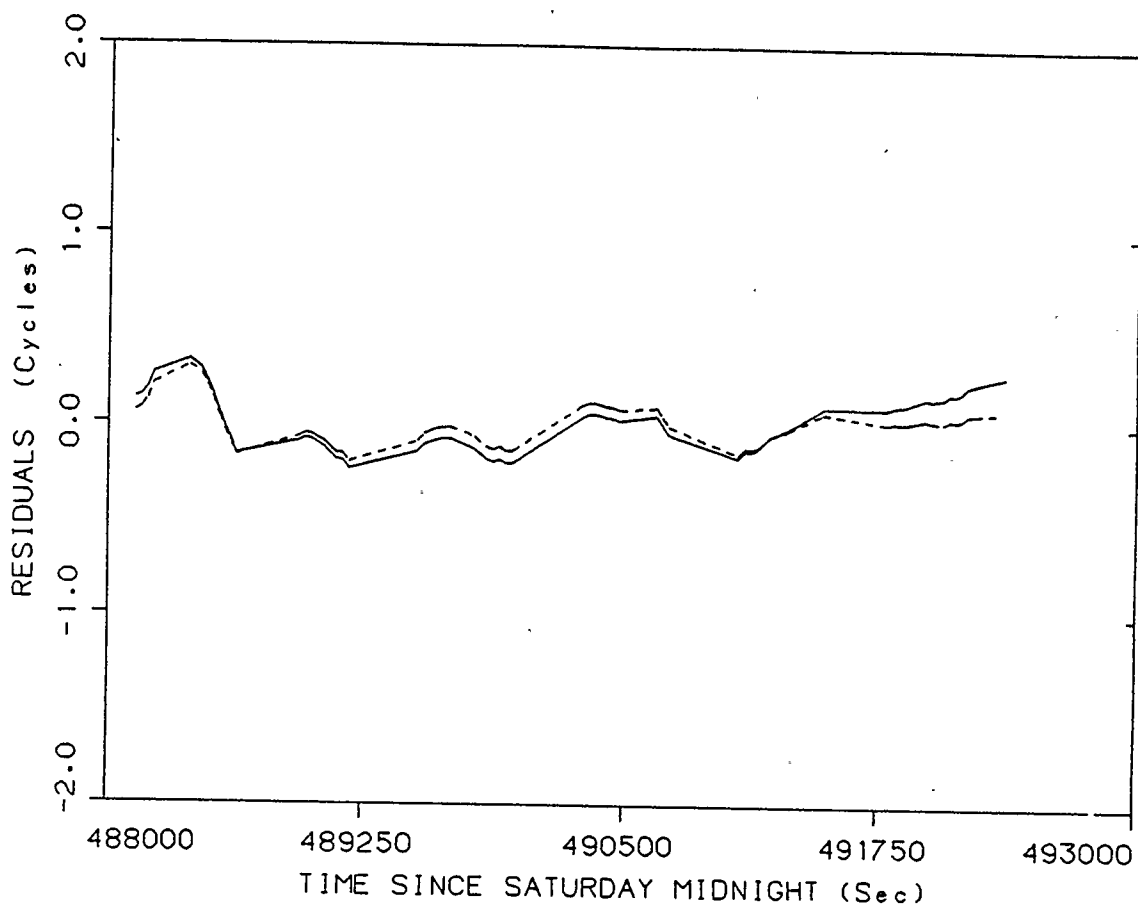


Figure 6.3: Comparison of the Residuals from  
Runs 6.2 and 6.3, Satellite Combination 13-11  
Solid Line Indicates Run 6.2 Residuals  
Dashed Line Indicates Run 6.3 Residuals

Utilizing polynomials to model the receiver clock error significantly weakens a double difference adjustment (Beutler et al., 1987). A preferred method, is to solve for

the clock offsets at each epoch with a single difference or single point adjustment. These corrections are then applied directly to the observations prior to performing the double difference adjustment (Beutler et al., 1987; Wei, 1986). This approach has not been attempted in this study but it is anticipated that this process will bring the results more in line with the TRIMBLE/TRIMVEC test results.

The results obtained from the two double difference versions are very similar. The simultaneous transmit time formulation of the ASTRO program package is therefore not a major contributing factor to the positioning errors. Weighted ambiguity double difference adjustments do not exhibit the same instability as the single difference adjustments. The convergence problem encountered in weighted ambiguity adjustments must be attributed to the single difference model.

## CHAPTER 7

### CONCLUSIONS AND RECOMMENDATIONS

The method of computing the Keplerian initial conditions directly from the broadcast ephemeris parameters has provided good results. Satellite positions determined by integrating the force model subject to the Keplerian initial conditions are within two metres of the satellite positions determined from the broadcast ephemeris. Preliminary estimates of the Keplerian initial conditions, derived directly from the broadcast ephemeris parameters, are improved by performing a least squares adjustment that fits the integrated orbit to the broadcast ephemeris orbit. No attempt is made to improve the estimate of the satellite positions at this time. If a more precise ephemeris is used to predict and correct the initial Keplerian elements, improvements in the estimated satellite positions can be expected.

An accurate initial estimate of the orbit is of prime importance if only a single baseline is being processed. The orbit improvement capabilities can only be utilized if data from a network of three or more stations with a spatial

extent of a few hundred kilometres or more is being processed. A network adjustment utilizing the orbit improvement capabilities of ASTRO should improve the satellite position accuracies.

The use of actual data in the original ASTRO program gave rather poor results. Large amplitude systematic trends are evident in plots of the residuals from adjustments which utilized only a polynomial receiver clock model. The systematic trend has been attributed to variations in the receiver clock offsets determined by the internal software of the receiver. Changes in the number of satellites tracked and satellite geometry give rise to the variations in the internally derived clock offsets. The instability of the quartz oscillator, used in the receiver, is shown in the residual plots by high frequency fluctuations superimposed on the systematic trend.

Remondi (1984) states that the receiver clock offsets must be known or modelled to an accuracy of less than one nanosecond in single difference adjustments. The amplitude of the systematic trend remaining in the residuals suggests that the initial versions of the ASTRO program package are not achieving this criterion.

Adding a first-order Gauss-Markov process to the polynomial clock model to remove the systematic trend has been only partially successful. Good adjustment results have been obtained only when the ambiguities are held fixed and short correlation times (120 seconds) are used in the Markov process. The correlation time derived from the autocorrelation function of the adjustment residuals lies within the range of 350 to 550 seconds. Adjustments using these longer correlation times removed most of the systematic trend but left a high frequency component, attributed to the oscillator fluctuations. Unfortunately, interaction between the Gauss-Markov process and the receiver clock polynomials prevents proper convergence of these adjustments. Reducing the correlation time to alleviate the interaction problem and absorb the higher frequency variations improves the convergence problems but does not completely correct them.

Entering an a priori estimate of the ambiguities provides a good initial starting value for the Markov process predictor. Treating the ambiguities as weighted parameters, to account for errors in their estimated values, results in adjustments that converge very slowly. The convergence problems occur on adjustments both with and without the Markov process incorporated.

Good adjustment results that are free of convergence problems have been obtained only when the ambiguities are held fixed and short correlation times (120 seconds) are used for the Markov process. The systematic trend still exists in the residuals but the amplitude is reduced from that of the initial adjustments.

Results from the two double difference adjustment programs indicate that the simultaneous transmit time and simultaneous received time models are essentially equivalent. As noted in Chapter 2, measuring the receiver clock offset at slightly different epochs should contribute only a negligible error to the bias modelling. The simultaneous transmit model will provide better results for orbit improvement. Both of the carrier phase observations used to form the single difference refer to the same satellite transmit time thus orbit improvement algorithms are more efficient.

The study seems to indicate that there is some inherent instability in the single difference model and that the methods implemented in this thesis have not successfully resolved it. The requirement of accurate a priori knowledge of the ambiguities significantly affects the usefulness of the processing scheme developed. In addition, it is felt that the receiver clock models currently implemented are not

the optimal solution to the clock problem. At present, the single difference models investigated in this thesis cannot be considered as a viable alternative to double difference adjustments.

Several additional methods of treating the receiver clock offsets have been proposed. The methods include:

- 1) Adding higher order terms to the receiver clock polynomial,
- 2) Utilizing piecewise continuous polynomials,
- 3) Removing predetermined values of the clock biases directly from the observations, and
- 4) Solving for the clock biases as a white noise process.

The first two methods attempt to reduce the magnitude of the systematic trend seen in the residuals. In the first method, higher order terms and/or cyclic components are added to the clock polynomials. In the second method, the length of piecewise continuous polynomials can be chosen to fit the pattern of the residuals. Both of these methods are difficult to justify physically. They are arbitrarily fitting functions to the observed pattern and do not deal with the physics of the problem. In addition, problems with

the interaction between the Markov process and the polynomials are likely to be aggravated.

The final two methods attempt to remove the actual receiver clock offset. In the third method, the clock biases can be determined at each epoch from a single point pseudorange solution. In view of the variability of pseudorange adjustments, this method will add a high degree of noise to the observations but the systematic trend will be removed. A Gauss-Markov process with short correlation times, in the single difference adjustments, may successfully reduce the noise level. Removing the clock offsets from the observations has proven successful in double difference adjustments where the noise level is reduced by forming the difference across satellites (Beutler et al., 1987a).

Solving for the receiver clock biases at each epoch will absorb the large systematic trend seen in the adjustment residuals. The neglected effect that arises from measuring the clock biases at each receiver at slightly different times should also be absorbed. The significant increase in the number of unknowns is a major disadvantage of this method, especially when simultaneously processing observations from a network of stations. With future

increases in computing power anticipated, this drawback may not be as significant in the future as it is right now.

Further research in this area is required to solve the receiver clock modelling problem and overcome the model instabilities.

## REFERENCES

- Arden, D.A.G. (1987) The Permanent Tide and Its Effects on the Deformable Earth. M.Sc. Thesis, Univ. Calgary, Dept. Surveying Engineering.
- Beutler, G., D.A. Davidson, R.B. Langley, R. Santerre, P. Vanicek and D.E. Wells (1984) Some Theoretical and Practical Aspects of Geodetic Positioning Using Carrier Phase Difference Observations of GPS Satellites. University of New Brunswick Technical Report No. 109.
- Beutler, G., I. Bauersima, W. Gurtner, M. Rothacher and T. Schildknecht (1987a) Evaluation of the 1984 Alaska Global Positioning System Campaign with the Bernese GPS Software. J. Geophys. Res., 92, B2, 1245-1303.
- Beutler, G., I. Bauersima, W. Gurtner, M. Rothacher and T. Schildknecht (1987b) Atmospheric Refraction and Other Important Biases in GPS Carrier Phase Observations. Paper presented at the XIX General Assembly of I.U.G.G, Vancouver, Canada, Aug. 9-22.
- Bock, Y., R.I. Abbot, C.C. Counselman and R.W. King (1986) A Demonstration of 1 - 2 Parts in  $10^7$  Accuracy Using GPS. Bull. Geod., 60, 241-251.
- Bock, Y., S.A. Gourevitch, C.C. Counselman, R.W. King and R.I. Abbot (1986b) Interferometric Analysis of GPS Phase Observations. Manuscripta Geodetica, 11, 282-288.
- Box, G.E.P. and G.M. Jenkins (1970) Time Series Analysis Forecasting and Control. Holden-Day, San Fransisco.
- Brown, R.G. (1983) Introduction to Random Signal Analysis and Kalman Filtering. John Wiley and Sons, New York.
- Brown, A.K. and M.A. Sturza (1985) Static Point Positioning with an L1, C/A Code Receiver, First Inter'l Symp. on Precise Positioning with GPS, Rockville, MD, 161-173.
- Buffett B.A. (1985) A Short-Arc Orbit Determination for the Global Positioning System. M.Sc. Thesis, The University of Calgary, Dept of Surveying Engineering, Report No. 20013.

- Campbell, J., T. Maniatis, A. Muller, and J. Vierbuchen (1986) On the Generation of Ionospheric Refraction Corrections for Single Frequency GPS Measurements. Fourth Inter'l Geodetic Symp. on Satellite Positioning, Austin Texas, 631-645.
- Clynch, J.R. and D.S. Coco (1986) Error Characteristics of High Quality Geodetic GPS Measurements: Clocks, Orbits and Propagation Effects. Fourth Inter'l Geodetic Symp. on Satellite Positioning, Austin Texas, 539-556.
- Conte, S.D. (1963) The Computation of Satellite Orbit Trajectories. Advances in Computers, 3, 1-76.
- Danby, J.M.A. (1962) Fundamentals of Celestial Mechanics, MacMillian, New York
- Davidson, J.M., C.L. Thornton, S.A. Stephens, S.C. Wu, S.M. Lichten, J. S. Border and O.J. Sovers (1986) Demonstration of the Fiducial Network Concept Using Data From the March 1985 GPS Field Test. Fourth Inter'l Geodetic Symp. on Satellite Positioning, Austin TX, 1019-1028.
- Davis, J.C. (1986) Statistics and Data Analysis in Geology. Second Edition, John Wiley and Sons, New York.
- Delikaraoglou, D., R.R. Steeves and N. Beck (1986) Development of a Canadian Active Control System Using GPS. Fourth Inter'l Geodetic Symp. on Satellite Positioning, Austin TX, 1189-1203.
- Delikaraoglou D. (1987) On Principles, Methods and Recent Advances in Studies Toward a GPS Based Control System for Geodesy and Geodynamics. NASA Technical Memorandum.
- Gelb, A. (1974) Applied Optimal Estimation. MIT Press, Cambridge, MA.
- Georgiadou, Y., and A. Kleusberg (1988) On the Effect of Ionospheric Delay On Geodetic Relative Positioning. Manuscripta Geodetica, 13, 1-8.
- Hilla, S.A. (1986) Processing Cycle Slips in Nondifferenced Phase Data From the Macrometer V-1000 Receiver. Fourth Inter'l Geodetic Symp. on Satellite Positioning, Austin TX, 647-661.

- Hopfield, H.S. (1971) Tropospheric Effect on Electromagnetic Measured Range: Prediction from Surface Data. Radio Science, 6, 3, 357-367.
- Hothem, L.D. and G.E. Williams (1985) Factors to be Considered in the Specifications for Geodetic Surveys Using Related GPS Techniques. First Inter'l Symp. on Precise Positioning with GPS, Rockville, MD, 633-644.
- Jenkins, G.M., and D.G. Watts (1968) Spectral Analysis and Its Applications. Holden-Day, San Francisco.
- Jones, A.C. and D.R. Larden (1987) First Order Geodetic Surveying Using Multi-Station Global Positioning Techniques. Presented at the Institution for Surveyors, Australia, 29th Australian Survey Congress, Perth, Australia, April 4-11.
- Jones, R.H. and P.V. Tryon (1987) Continuous Time Series Models for Equally Spaced Data Applied to Modelling Atomic Clocks. SIAM J. Sci. Stat. Comput., 8, 1, 71-81.
- Kaula, W.M. (1966) Theory of Satellite Geodesy. Blaisdel Publ. Waltham, Mass
- King, R.W., E.G. Masters, C. Rizos, A. Stolz and J. Collins (1985) Surveying With GPS. Monograph No. 9, School of Surveying, Univ. New South Wales, Kensington, Australia.
- Kleusberg, A. (1986) Ionospheric Propagation Effects in Relative GPS Positioning. Manuscripta Geodetica, 11, 256-261.
- Klobuchar, J.A. (1982) Ionospheric Corrections for the Single Frequency User of the Global Positioning System. Proc. National Telecommunications Symp., Nov. 7-10, Galveston, TX.
- Lachapelle, G. and M.E. Cannon (1986) Single and Dual Frequency GPS Results for Baselines of 10 to 500 km. The Canadian Surveyor, 40, 2, 173-183.
- Langley, R.B., G. Beutler, D. Delikaraoglou, B. Nickerson, R. Santerre, P. Vanicek and D.E. Wells (1984) Studies in the Application of the Global Positioning System to Differential Positioning. Tech. Rep. 10, Dept of Surveying Engineering, Univ. of New Brunswick, Fredericton, N.B.

- Langley, R.B., D. Parrot, R. Santerre, P. Vanicek and D.E. Wells (1986) The Spring 1985 GPS High-Precision Baseline Test: Preliminary Analysis with DIPOP. Fourth Inter'l Geodetic Symp. on Satellite Positioning, Austin Texas, 1073-1088.
- McArthur, D. (1987) Report on Test Results with the TRIMBLE NAVIGATION 4000SX Surveyor. Geodetic Survey of Canada Tech. Report No. 9.
- Moritz, H. and I.I. Mueller (1987) Earth Rotation, Theory and Observations. Ungar Publishing, New York.
- Nakiboglu S.M., E.J. Krakiwsky, K.P. Schwarz, B.A. Buffett and B.A. Wanless (1985) A Multi-Station, Multi-Pass Approach to Global Positioning System Orbit Improvement and Precise Positioning. Geodetic Survey of Canada Contract Report No. 85-003.
- Pointon, K.W., I.N. Tziavos, M.E. Cannon, T. Yokokura, E.J. Krakiwsky and K.P. Schwarz (1987) Implementation of GPS Model Improvements for Geophysical Applications. Presented at the XIX General Assembly of the IUGG, Vancouver, Canada, Aug. 9-22.
- Remondi, B. (1984) Using the Global Positioning System (GPS) Phase Observable for Relative Geodesy: Modelling, Processing and Results. Ph.D. Dissertation, Center for Space Research Report CSR-82-2, University of Texas, TX
- Swift, E.R. (1985) NSWC's GPS Orbit/Clock Determination System. First Inter'l Symp. on Precise Positioning with GPS, Rockville, MD, 51-62.
- Skrumeda, L.L. and S.A. Stephens (1987) Stochastic Colored-Noise Estimation of Clocks and Tropospheres in Analysis of GPS Geodetic Data. Presented at the XIX General Assembly of the IUGG, Vancouver, Canada, Aug. 9-22.
- Tralli, D.M., T.H. Dixon and S.A. Stephens (1988) Effect of Wet Tropospheric Path Delays on Estimation of Geodetic Baselines in the Gulf of California Using the Global Positioning System. J. Geophys. Res., 93, 6545-6557.
- Tziavos, I.N. (1987) Cycle Slips Software. University of Calgary, Department of Surveying Engineering Internal Report.

- Van Dierendonck, A.J., S.S. Russel, E.R. Kopitzke and M. Birnbaum (1980) The GPS Navigation Message. Global Positioning System: Papers Published in Navigation, Vol. 1, The Institute of Navigation, Washington, D.C.
- Vanicek, P., G. Beutler, A. Kleusberg, R.B. Langley, R. Santerre and D. Wells (1985) DIPOP: Differential Positioning Program Package for the Global Positioning System. Final Report for DSS Research Contract No. OST 83 - 00353, Dept. Surv. Eng., Univ. New Brunswick.
- Vanicek, P., and E.J. Krakiwsky (1986) Geodesy: The Concepts. Second Edition, North-Holland, Amsterdam.
- Wanless, B.A. (1985) A Prototype Multi-Station, Multi-Pass GPS Data Reduction Program. M.Sc. Thesis, The University of Calgary, Dept of Surveying Engineering, Report No. 20014.
- Wanless, B.A., and G. Lachapelle (1988) NOVAS - an Automated Program for the Precise Reduction of GPS Carrier Phase Observations. Manuscripta Geodetica, 13, 201-209.
- Wei, Z. (1985) GPS Positioning Software at the Ohio State University: Franklin County Results. First Inter'l Symp. on Precise Positioning with GPS, Rockville, MD.
- Wei, Z. (1986) Positioning with NAVSTAR, the Global Positioning System. Rep. No. 370, Dept. Geodetic Science and Surveying, Ohio State University, Columbus.
- Wells, D., D. Delikaraoglou, A. Kleusberg, E.J. Krakiwsky, G. Lachapelle, R.B. Langley, M. Nakiboglu, K.P. Schwarz, J.M. Tranquilla and P. Vanicek (1986) Guide to GPS Positioning. Canadian Institute of Surveying and Mapping, P.O. Box 5378, STN F, Ottawa, Ontario.
- Yule, G.U. and M.G. Kendall (1950) An Introduction to the Theory of Statistics. 14-th Edition, Hafner, New York.

## APPENDIX A

The following table gives a brief description of each adjustment along with the page numbers of the table that lists the station coordinate errors. Unless otherwise noted, the adjustments refer to the baseline ROOF to CATA.

Run #	Page	Description
4.1	51	Baseline ROOF to CATA, full data set, 60 second spacing, station (stn) coordinate (coord) convergence (conv) 0.001 m in 3 iterations, stn variance (var): 25 m <sup>2</sup> , ambiguities (amb): free.
4.2	51	Baseline ROOF to METC, same as run 4.1.
4.3	51	Baseline METC to CATA, same as run 4.1.
5.1	59	Baseline ROOF to CATA with updated clock model.
5.2	59	Baseline ROOF to METC with updated clock model.
5.3	59	Baseline METC to CATA with updated clock model.
5.4	59	Repeat run 5.1 with fixed ambiguities.
5.5	59	Repeat run 5.1 with the constant term of the receiver clock polynomial (d <sub>0</sub> ) fixed.
5.6	59	Baseline ROOF to CATA, adjusting only the data with five satellite coverage.

- 5.7 69 Repeat run 5.5 with weighted ambiguities, convergence at 0.004 m in 17 iterations.
- 5.8 69 Repeat run 5.7 while solving for the  $d_0$  term.
- 5.9 79 Repeat run 5.7 with a Gauss-Markov process model incorporated. A priori weighted of clock polynomial coefficients increased. Convergence at 0.020 m in 21 iterations.
- 5.10 79 Repeat run 5.8 with a Gauss-Markov process and increased weights of clock polynomial coefficients. Conv. at 0.040 m in 11 iter.
- 5.11 79 Repeat run 5.9 with correlation time reduced to 120 sec. Conv. at 0.010 m in 21 iter.
- 5.12 79 Repeat run 5.11 with fixed amb. Conv. at 0.002 m in 8 iter.
- 5.13 79 Repeat run 5.12 while solving for the  $d_0$  term.
- 5.14 79 Baseline ROOF to METC with Gauss-Markov process and fixed amb. Equivalent to run 5.13.
- 5.14 79 Baseline METC to METC with Gauss-Markov process and fixed amb. Equivalent to run 5.13.
- 6.1 83 Version 1 double difference adjustment solving for stn coord and amb only. Conv: 0.001 m in 2 iterations.
- 6.2 89 Version 2 double difference adjustment solving for stn coord and amb as free parameters. Conv: 0.001 m in 3 iterations.
- 6.3 89 Repeat run 6.6 with poly to model receiver clock errors and tropospheric scale factor incorporated. Conv: 0.001 m in 4 iterations.